Integrated Master in Chemical Engineering

Passive Direct Ethanol Fuel Cells for portable applications: experimental studies

Master Thesis

Inês Figueiredo Carviçais

Dissertation developed within the curricular unit of Dissertation
at the Faculty of Engineering, University of Porto

Supervisor: Doctor Alexandra Maria Pinheiro da Silva Ferreira Rodrigues Pinto

Associated Professor at Chemical Engineering Department

Co-supervisor: Doctor Vânia Sofia Brochado de Oliveira

Post-doctoral Researcher at Chemical Engineering Department

Universidade do Porto

Faculdade de Engenharia

FEUP

Chemical Engineering Department
Laboratory E206 – CEFT : Transport Phenomena Research Center

July, 2015

Acknowledgements

It's always very difficult to thank every single person that helped me and supported me on this journey, without them I don't know if I had been able to overcome all the obstacles and insecurities that appeared along the way.

Since I cannot thank to you all individually I am going to address my most sincere acknowledgements to those who were more important.

To my family, mom, dad, sister, grandma Lisa and grandma Lina that were always there for the good and the bad moments I thank you all for the advice, incentive and comforting words on the end of each day.

To my friends Ana Moreira and Patrícia Cruz (Ruby) thanks for making me company in all those lunches and for the talks during the coffee break.

I would like to thank to Professor Alexandra Pinto and to Vânia Oliveira for giving me the opportunity of writing this thesis which made me realize that research work is something that I want to pursue in the future. I also would like to thank to Salomé Soares, from the Laboratory of Catalysis and Materials, for the all the time spend preparing the catalysts that represent a very important part of this thesis.

Finally, I could not help but to thank to Maria João Cunha, my longtime best friend, for always being there and for putting up with me all these years, and to Pedro, my boyfriend, for the support, the patience, the friendship, the affection and last but not least for the love.

Abstract

The energetic demand grows each day due to the fast technological evolution. To keep up with this rapid development we must find new ways of producing energy preferably in an environmental friendly and renewable way. The DFECs (direct ethanol fuel cells) fit perfectly into this profile since they use ethanol as fuel, which can be produced from biomass, and are a low carbon dioxide emissions technology.

This thesis was focused on the study of passive DEFCs in order to optimize their performance by testing different combinations of fuel cell components in order to take a step towards to its commercialization.

It was used a passive DEFC with an active area of 10.2 cm^2, a Nafion 117 membrane and stainless steel connector plates. In this experimental study the parameters analysed were the cathode thickness and catalyst loading, the anode diffusion layer material, the catalysts materials, metal percentage and loading, and the operating parameter studied was the ethanol concentration.

The analysis of the results reported that the best ethanol concentration depends on the anode diffusion layer so, for carbon cloth it must be used a 3 M and for carbon paper a 2 M ethanol solution. In terms of the cathode side the highest catalyst loading, 1 mg/cm^2, and the thicker carbon paper diffusion layer, 0.400 mm, demonstrated the best results. Regarding the anode side several binary catalysts were tested in different diffusion layer materials and with different loadings and the results showed that the 40% Pt-40% Sn/20% CB catalyst with a loading of 3 mg/cm^2 and the carbon cloth, with a thickness of 0.400 mm, was the configuration that ensures the best performance.

Two ternary anode catalysts were tested and even though the performance of these catalysts didn't achieved the power density values of the 40% Pt-40% Sn/20% CB catalyst the 24% Pt-12% Sn-4% Ni /60% CB catalyst showed similar results.

Keywords: Passive direct ethanol fuel cell, ethanol oxidation, anode catalyst, design parameters, ethanol concentration, optimization.

Resumo

A procura energética aumenta de dia para dia devido à rápida evolução tecnológica. Para conseguir acompanhar este desenvolvimento é preciso encontrar novas maneiras de produzir energia de forma renovável e amiga do ambiente. As células de combustível a etanol encaixam perfeitamente neste perfil uma vez que, utilizam etanol como combustível, sendo que este pode ser produzido a partir da biomassa, e são uma tecnologia com baixas emissões de dióxido de carbono.

Esta tese focou-se na otimização de células de combustível com alimentação passiva de etanol testando várias combinações de diferentes componentes de forma a dar um passo em frente no que toca á sua comercialização.

A célula de combustível com alimentação passiva a etanol utilizada neste estudo possuía uma área ativa de 10,2 cm^2, uma membrana de Nafion 117 e placas coletoras de aço inoxidável. Neste trabalho experimental foram analisados os seguintes parâmetros: espessura e carga do catalisador do cátodo, material da camada difusiva do ânodo, percentagem de metal e carga do catalisador do ânodo e concentração de etanol.

A análise dos resultados mostrou que a melhor concentração de etanol depende da camada difusiva do ânodo sendo que, para o tecido de carbono deve ser utilizada uma solução de etanol de 3 M e para o papel de carbono de 2 M. No lado do cátodo a maior carga de catalisador, 1 mg/cm^2, e camada difusiva mais grossa de papel de carbono, 0,400 mm, foi a combinação que atingiu melhores resultados. No que toca ao lado do ânodo vários catalisadores binários foram testados em diferentes camadas difusivas com diferentes cargas, os resultados obtidos mostraram que a configuração que obteve um melhor desempenho foi o tecido de carbono, com uma espessura de 0,400 mm e com uma carga de 3 mg/cm^2 do catalisador 40% Pt-40% Sn/20% CB.

Dois catalisadores ternários foram testados e ainda que, o desempenho de ambos não tenha alcançado os valores de densidade de potência obtidos com o catalisador 40% Pt-40% Sn/20% CB, o catalisador 24% Pt-12% Sn-4% Ni /60% CB foi o que obteve os resultados mais próximos.

Palavras-chave: célula de combustível com alimentação passive de etanol, oxidação do etanol, catalisador do ânodo, parâmetros configuracionais, concentração de etanol, otimização.

Declaration

I declare, on oath, that this work is original and that all the not original contributions are appropriately identified with the respective source.

_____

(Inês Figueriredo Carviçais)

Table of Contents

List of Figures

List of Tables

Nomenclature

- E – real fuel cell voltage (V)
- E_{cell} – thermodynamic equilibrium potential (V)
- F – Faraday's constant ($C.mol^{-1}$)
- G – Gibbs free energy ($kJ.mol^{-1}$)
- H – enthalpy of reaction ($kJ.mol^{-1}$)
- i – current density ($A.cm^{-2}$)
- i_{cell} – cell current density ($A.cm^{-2}$)
- i_{C2H5OH} – leakage current density due to ethanol crossover ($A.cm^{-2}$)
- n – number of electrons
- P – power density ($W.cm^{-2}$)
- V – voltage (V)
- W_{elec} – maximum electrical work potential ($kJ.mol^{-1}$)

Greek

- Δ – Variation
- ε_{fuel} – fuel efficiency
- ε_{real} – total efficiency
- ε_{thermo} – thermodynamic efficiency
- $\varepsilon_{voltage}$ – voltaic efficiency

Acronyms

- AFC – Alkaline Fuel Cell
- CB – Carbon Black
- CC – Carbon Cloth
- CCM – Catalyst-coated Membrane
- CEFT – Centro de Estudos de Fenómenos de Transporte
- CP – Carbon Paper
- DAFC – Direct Alcohol Fuel Cell
- DEFC – Direct Ethanol Fuel Cell
- DMFC – Direct Methanol Fuel Cell
- FEUP – Faculdade de Engenharia de Universidade do Porto
- GDL – Gas Diffusion Layer
- GW – Gigawatt

LCM – Laboratory of Catalysis and Materials

MEA – Membrane Electrode Assembly

MCFC – Molten Carbonate Fuel Cell

MPL – Microporous Layer

NASA – National Aeronautics and Space Administration

OCV – Open Circuit Voltage

PAFC – Phosphoric Acid Fuel Cell

PEM – Proton Exchange Membrane

PEMFC – Proton Exchange Membrane Fuel Cell

PTFE – Polytetrafluoroethylene

SOFC – Solid Oxide Fuel Cell

1. Introduction

1.1. Motivation

Electricity is an energy resource long used by humans. Its discovery dates back to the Ancient Greece although its practical application was not found until mid-eighteenth century. Ever since, electricity has been on the basis of the development of modern societies wherein, much of the technology that currently moves the world uses this energy source.

These days in order to meet the electricity demand which is growing at a rapid rate due to the heavy technological development, it is necessary to study more sustainable ways to produce energy in order to reduce fossil fuel dependency. Using less fossil fuels is crucial to decrease the air pollution since the combustion of fossil fuels releases carbon dioxide and other greenhouse gases, so, to cover the electricity demand it is essential to proceed with the study of other ways of electrical power production.

The consequences of air pollutants emissions are the global warming, the ozone layer depletion and the acidic rain so, it's very important to follow the basic measures suggested in Kyoto's Protocol. This protocol includes three important rules but there is one that fits better the context of this work which is the encouragement of using low gas emission technologies.

Among the different energy conversion technologies fuel cells are very promising since they produce very small amounts of carbon dioxide and in some cases, along with electricity, they can produce heat allowing them to be integrated in cogeneration systems. Fuel cells are also good candidates to replace the internal combustion engines or to supply energy to mobile, portable, or stationary applications.

Fuel cells, namely the ones who work with alcohol as fuel (DAFCs), possess some advantages such as easy handle and transport of the fuel, as it is liquid at room temperature, and easy refuelling of the cells. The most promising alcohols are methanol, ethanol and 2-propanol due to their high energy density. Fuel cell devices work as modular structures, have great autonomy and the conversion of chemical energy into electric energy is very reliable.

1.2. Objectives and Thesis Layout

The main objective of this thesis is to optimize the performance of a passive DEFC in order to reach the power density levels that can satisfy the needs of small portable electronic devices by changing some of the fuel cell components such as, the anode catalyst, the cathode catalyst, the gas diffusion layer materials and the ethanol concentration fed to the cell.

This thesis is organized in six chapters and a brief description of the content of each chapter is written below.

The first Chapter provides a general perspective of the relevance of this work.

Chapter 2 is dedicated to the description of fuel cell devices, their historic evolution, and has an overview on the fuel cell types and provides a perspective of their global market.

The Chapter 3 is devoted exclusively to direct ethanol fuel cells and provides a description of their working principle, the advantages and disadvantages, the possible applications, as well as, the state of the art of this technology.

In Chapter 4 can be found all the experimental set up: the fuel cell components and the equipment used to perform the tests and the experimental procedure.

Chapter 5 contains all the experimental results along with the respective discussion. And finally, on Chapter 6 the conclusions of this work, as well as, some suggestions to further investigation, are presented.

2. Fuel Cells

Fossil fuels pose both environmental and shortage issues, which combined with the accentuated growth and development of modern societies led the scientific community to seek alternatives to the conventional power production.

Among the possible alternatives, fuel cells appear to be good candidates to replace already existing applications of heat and electric generation since their operation entails lower environmental impact, in terms of low CO_2 (carbon dioxide) emissions, benefiting the environment, and in some cases their fuel can even be produced from renewable sources.

Current studies on fuel cell technology aim to reduce energy losses during energy conversion process to increase their performance and to make this technology more attractive to the global market.

2.1. Description of Fuel Cells

Fuel cells are electrochemical devices that continuously convert the chemical energy contained in the fuel into electrical power (generating some heat in the process), as long as fuel and oxidant are available [2]. The majority of fuel cells use hydrogen as fuel however, there are certain types of cells that can operate with other fuels as long as they are rich in hydrogen. The oxidant is always the oxygen normally provided by the air [3, 4].

Typically a fuel cell is a combination of an electrolyte, a pair of electrodes, the anode and the cathode, and an external circuit [4, 5].

At the electrodes the half-reactions that comprise the electrochemical global reaction take place. These consist on the fuel oxidation, at the anode and the reduction of the oxidant, at the cathode, and are generally represented by Equations 2.1 and 2.2.

$$\text{Oxidation reaction:} \quad \text{Fuel} \rightarrow \text{Protons} + \text{Electrons} \tag{2.1}$$

$$\text{Reduction reaction:} \quad \text{Oxidant} + \text{Protons} + \text{Electrons} \rightarrow \text{Water} \tag{2.2}$$

The electrolyte acts not only as a separating element of the anode and cathode compartments but also as the ion (protons) transport element and should behave as an electronic insulator to prevent electrons from going through the electrolyte, forcing them to flow through the external circuit, performing electrical work [6].

The electric production capacity of a cell is directly related to its active area, therefore a higher active area will have a higher number of active sites where the reaction occurs therefore more electrons will be produced and will flow through the external circuit. To maximize the electrode area per volume ratio they must have flat configurations and should be highly porous [6]. In most cases

reactions are favoured by the presence of a catalyst layer whose function is to lower the activation energy of the reaction.

Once known the elements of a fuel cell and the reactions involved in its operation it is also important to understand the energy conversion mechanism. The transformation of chemical energy into electrical energy involves only one step, the electrochemical reaction, although the energy conversion involves four stages (Figure 2.1) [6]:

① **à** Transport of reactants: the fuel and oxidant are provided to the cell on the anode and on the cathode side, respectively. The constant supply of reactants can become a difficult task when the cell operates at high currents due to higher consumption rates on this case. For this reason the materials and the design of the layers responsible for reactants distribution are very important to the performance of the cell.

② **à** Electrochemical reaction: the half-reactions release/consume electrons and ions. The ions and electrons are generated on the anode and consumed on the cathode. The electron flux through the external circuit generates electrical current which is directly related to the rate at which the reactions proceed so, greater currents require higher reaction rates. The use of catalysts raises the rate and the efficiency of the electrochemical reactions. Therefore, the choice of the catalyst to be used in the cell is crucial to achieve good performances.

③ **à** Transport of ions and electrons: the transport of these two species is performed by the establishment of an electrical gradient. These are natural phenomena that occur in an attempt to balance the loads between the two sides of the cell. Electrons flow quite easily through the external circuit since it is built with materials that are good electrical conductors. However, the ions transport tends to be more difficult since they have to pass through the electrolyte to reach the other electrode. The crossing mechanism of ions can be described as if they were jumping from one molecule of electrolyte to another, having for that reason a higher transport resistance.

④ **à** Removal of the reaction products: besides electricity there are other products that result from the electrochemical reactions, for example in DAFCs (Direct Alcohol Fuel Cells) reactions water and CO_2 are produced. To provide a smooth operation of the cell it is necessary to remove these compounds from the reactional environment otherwise they would accumulate inside the cell. Fortunately, the removal process uses the same mechanism as reactants distribution described in step ①. To certain types of cells, such as PEMFCs (Polymer Electrolyte Membrane Fuel cells), this step can be very important in order to prevent flooding of the cathode [6].

The performance of a fuel cell can be evaluated by their polarization curve also known as V-i curve. This curve consists on the representation of the voltage (V), expressed in Volt, as a function of current density (i), expressed in Ampère per square centimetre (A/cm^2) (Figure 2.2) It is very important that the current is expressed in terms of area in order to compare the performances of cells with different active areas [6].

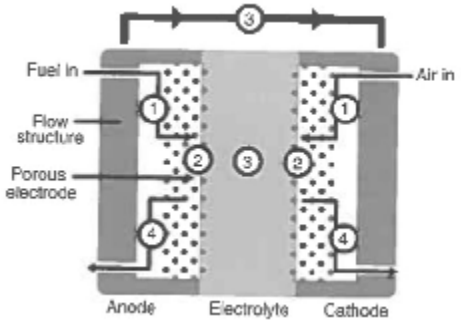

Figure 2.1: Cross section of a fuel cell [6].

Applying Equation 2.3 it is possible to calculate the power density (P), expressed in Watt per square centimetre (W/cm^2). The plot of the power density as a function of current density is called the power density curve (Figure 2.2) [6].

$$P = i.V \tag{2.3}$$

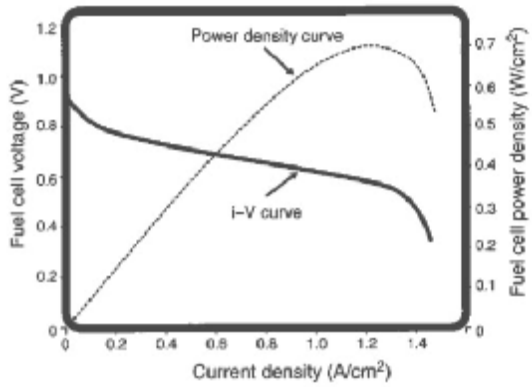

Figure 2.2: Combined fuel cell i-V and power density curves [6].

Figure 2.2 shows the standard shape of both V-i and power density curves. The V-i curve shows that the voltage decreases whenever the current density increases. However, in ideal conditions the fuel cell should be able to provide a constant voltage, determined by thermodynamics, regardless the current density (Figure 2.3). Real cells cannot maintain a constant voltage due to physical and energetic barriers, which represent irreversible energy losses, causing the actual voltage of the cell to be lower than ideal one, predicted by thermodynamics [6].

Depending on the operating current density there are three types of losses: activation losses, ohmic losses and mass transfer losses, each one having a higher impact, respectively, at low, medium and high current densities (Figure 2.3) [6].

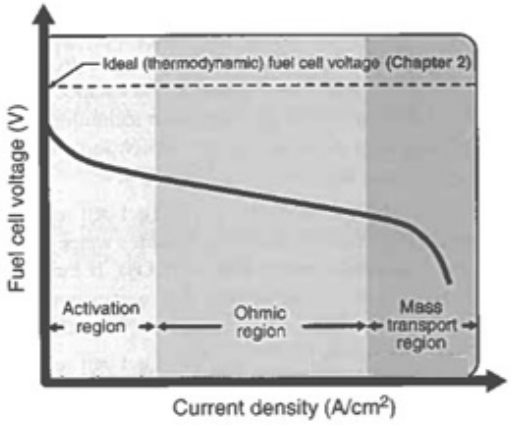

Figure 2.3 : Schematic representation of a typical fuel cell i-V curve and the thermodynamically predicted voltage [6].

Activation losses are related to the energy that is needed to overcome the activation barriers to begin the electrochemical reactions. The ohmic losses follow the Ohm's law and are due to the resistance of the ionic and electronic conduction. At last, the mass transfer losses occur when the consumption rate of reactants is very fast which may lead to the depletion of reactants or to the accumulation of products near the catalyst layer causing accentuated energy losses [6].

Fuel cells and batteries share some common characteristics such as their energy conversion principle, however, the main difference between these two types of technology is their operating period. For batteries the operating time is determined by the reactants storage capacity that restricts the power production, since once it runs out of reactants the battery will not be able to provide more energy. In the case of fuel cells that does not exist since it is possible to extend its operation period through the continuous supply of fuel and oxidant [6, 7].

The advantages of fuel cells are related to their straightforward energy conversion mechanism, the possibility of working for extended periods, the low gas emissions, the nonexistence of moving parts, which reduces maintenance costs, to their modular structure and quiet operation, since no noise or vibrations are emitted [6, 8].

Significant irreversible losses, high operating temperatures, short life time, high production costs and in some cases the need of gas storage are the main disadvantages of fuel cells when comparing them with batteries or internal combustion engines [6, 8].

Nevertheless, when balancing the advantages and disadvantages of the fuel cell technology it can be concluded that the advantages outweigh the disadvantages, otherwise there was no justification to the growing research on this technology.

2.2. Historic Evolution

Fuel cells were only named this way in 1922 by Rideal and Evans before that they were called gas voltaic batteries.

Experiments concerning the working principles of these batteries were first conducted in 1838 by the German chemist Christian Friedrich Schöenbein. Although he was the first one to work with that he was not their father, this role belongs to Sir William Robert Grove. In 1839 he put together a cell composed by two electrodes half submerged in an aqueous solution of sulphuric acid, the electrolyte, two inverted tubes over the electrodes, one containing hydrogen and the other containing oxygen. This cell was able to produce low currents but only for a short period of time [2]. Later Grove put in series 26 cells in order to supply sufficient energy to perform water electrolysis using its own products, hydrogen and oxygen, as the power source.

In 1843 he suggested that his cell was used as an eudiometer, a device that measures the volumetric composition of a gas mixture, usually used to assess air quality due to its sensibility to oxygen [2, 9]. It wasn't until 1854 that Grove proposed the use of his cell as an energy source [2].

In 1882 Lord Rayleigh developed a new gas battery, with a different configuration, that was fed with coal gas, however his results were no better than Grove's.

In 1889 Ludwig Mond and Carl Langer improved Rayleigh's battery by solving the flooding problems in both electrodes caused by the liquid electrolyte. Later that year they presented their improved prototype at the Royal Society of London's convention which didn't go unnoticed to the eyes of Alder Wright and Thompson that had been working with a similar battery, which they called aired plates, since 1887.

Aired plates were devices made of porous non-conductive plates coated with platinum black on the aerated side and on the opposite side, where the hydrogen gas was enclosure, the plate was made of an oxidizable material. The electrolyte was a solution of sulphuric acid absorbed in a porous material. The maximum voltage obtained with a double aerated plate cell was between 0.6 and 0.7 V, and its poor performance was caused by the difficulty of keeping the hydrogen from leaking.

The understanding of the relationship between the components of the fuel cell: electrode, electrolyte, reduced and oxidated agents, anions and cations was determined experimentally by Friedrich Wilhelm Ostwald in 1893. His theory, which involves both physical and chemical concepts, confirmed the assumptions made by Grove therefore, solving the puzzle of the gas voltaic battery [2].

At the end of the nineteenth century, Mond, Langer and Ostwald believed that hydrogen could become, in the twentieth century, the most widely used fuel replacing coal , beginning the "Age of Electrochemical Combustion" where conventional internal combustion engines would be replaced by fuel cells with higher efficiencies and lower gas emissions [9].

Already in the 30s, Francis Thomas Bacon developed the first cell of hydrogen and oxygen with practical application. During World War II, Bacon was involved in the development of a fuel cell that

was used in submarines of the Royal Navy. Later, in 1959, he joined the group of scientists responsible for the Apollo spacecraft design, developing, in partnership with Marshall Aerospace company, a cell using common metals and with high voltage and current density, with an efficiency of 60% [9].

In 1950 appeared on the market a new material called Teflon (polytetrafluoroethylene or PTFE) and was employed on fuel cells in order to control the water flow through the electrolyte and avoid the cathode flooding. Five years later, a chemist of General Electric Company proposed the use of a sulfonated polystyrene membrane as a solid electrolyte. Niedrach Leonard who worked for the same company, in 1958, placed over the membrane a layer of platinum in order to catalyze the oxidation and reduction reactions [9].

In the late 60s, DuPont brought to the market a material called Nafion®. Researchers used this material, a sulfonated polymer, as the proton exchange membrane which revealed good results. Since then Nafion® became the most used material to be used as proton exchange membranes [8].

The first experiments with direct methanol fuel cells were carried out in 1990 by Jet Propulsion Laboratory of NASA in collaboration with the University of Southern California [9].

The year 2000 was an important milestone in the history of fuel cells as it marked the beginning of their commercialization [8].

More recently, fuel cell research is also focused on the use of other alcohols, besides methanol, as fuel, such as ethanol, ethylene glycol and 2-propanol [1]. Apart from using different alcohols, researchers are also studying the behaviour of the cells when they are fed with mixtures of different alcohols such as mixtures of methanol and ethanol.

2.3. Types of Fuel Cells

Fuel cells differ on the materials used on electrodes, on the fuel, on the electrolyte and on the operating conditions, however, the principle inherent to their operation is always the same.

Because they share the same working principle there are several common advantages to all fuel cell types: silent operation and environment friendly, since they have low CO_2 emissions and generally, besides electricity, the main product of the electrochemical reaction is water.

Fuel cells are classified according to their electrolyte: PEMFCs, AFCs, PAFCs, SOFCs, MCFCs e DAFCs [4]. This classification determines the electrochemical reactions, the catalyst used, the operating temperature, the fuel required, the applications and the efficiency.

In the next sub-chapters advantages and disadvantages for each type of fuel cells are noted, as well as, their main characteristics and applications. Specific information regarding the different fuel cell types can be found in Table A.1 on Appendix A.

2.3.1. Proton Exchange Membrane Fuel Cells (PEMFCs)

PEMFCs are robust, compact, with a simple design without moving parts and with a solid and non-corrosive electrolyte. All these reasons show that these don't require much maintenance and that their production cost is low. The major problem of this type of fuel cell is its life time since it remains quite low [4, 9].

PEMFCs are tolerant to CO_2 presence, making possible to use air as the oxygen source thus, lowering the operational costs [6, 8].

Temperature influences the energetic efficiency of these fuel cells thus, increasing the temperature will increase the efficiency. However, operating temperatures cannot be over 100ºC because since this is the boiling point of water, water can evaporate and dehydration of the membrane may occur. These membranes need a certain water content to work right so, when dehydrated they can lead to problems in terms of protons transport [4].

PEMFCs have a wide range of possible applications such as transports, portable devices and as backup systems [4].

2.3.2. Alkaline Fuel Cells (AFCs)

AFCs are rather light and small, their electrolyte, usually liquid potassium hydroxide (KOH), is not expensive and their catalyst is made of non-precious metals lowering the production cost. Although cheaper, the electrolyte is corrosive which reduces the life time of these cells [6, 8, 9].

In AFCs the CO_2 tolerance is extremely small because CO_2 combines with KOH to form potassium carbonate (K_2CO_3) leading to the deterioration of the electrolyte, so the electrolyte needs to be replaced periodically. To assure the preservation of the cells they must be fed with pure H_2 and pure O_2, increasing their costs of operation. Another problem is the water production on the anode side that occurs at twice the speed of its consumption on the cathode diluting the electrolyte and decreasing the performance if not properly removed [4, 6, 9].

This type of fuel cells was first used by NASA, as part of the Gemini and Apollo space programs, to provide water and power to astronauts. Nowadays they are used on boats, on submarines and military equipment as power suppliers [4, 6].

2.3.3. Phosphoric Acid Fuel Cells (PAFCs)

PAFCs are made of a low-cost electrolyte but their production cost is relatively high due its platinum carbon supported catalyst [4, 6].

Its electrolyte is corrosive and is a liquid in a range of temperature between 160 and 220ºC but its melting point is near the 40ºC which is a problem at the start-up. The high operating temperatures cause the evaporation of the electrolyte during the operation period [4, 6].

The tolerance for the fuel and oxidant impurities is high which represents a great advantage in terms of operating conditions [4, 6].

PAFCs are a mature and reliable technology and are widely used in stationary and space applications. Their integration in industrial environments is a beneficial since the production of electricity is associated with heat release [4, 8].

2.3.4. Solid Oxide Fuel Cells (SOFCs)

These cells have a solid electrolyte and the catalyst is made of non-precious metals however, its production cost is high due to the need of using materials capable of withstanding very high temperatures [6, 8, 9].

The high operating temperatures allow them to be part of co-generation systems which increases the overall efficiency of the cells. Nevertheless, these temperatures pose serious problems concerning the cell's initiating and cooling cycles. Efforts have been made in order to avoid these problems because it is believed that in the future the energy production may require the use of this technology [4].

Although SOFCs have moderate tolerance for sulphur, as well as MCFCs, they have a great advantage because they can work using a wide variety of different fuels [6].

The use of this type of cells is reduced to stationary applications [4].

2.3.5. Molten Carbonate Fuel Cells (MCFCs)

These fuel cells electrolyte is a mixture of molten carbonate salts and their catalyst is made of non-precious metals. MCFCs present a great flexibility relatively to the fuel and this is the reason why these cells stand out from other types of fuel cells [4].

In this technology, in addition to the reduction and oxidation reactions, occur methane and carbon monoxide reforming reactions.

The corrosive effect of the molten electrolyte, the dissolution of the catalysts in the electrolyte and the electrolyte losses by evaporation lead to high maintenance costs [6, 8].

This technology is appropriate for large-scale applications and is able to integrate into co-generation systems due to its high range of operating temperatures.

MCFCs are often employed in the industry and in military projects [4, 6].

2.3.6. Direct Alcohol Fuel Cells (DAFCs)

DAFCs are similar to PEMFCs because they have the same structure. Generally these cells use the same type of proton exchange membrane and electrolyte and the main difference between them is the fuel supplied to the cells [1].

The features shared between these two types of cells give to DAFCs some of the PEMFCs advantages such as being compact and robust, having a simple design without moving parts and also having a solid non-corrosive electrolyte which have low maintenance needs.

Alcohols like methanol, ethanol, ethylene glycol and 2-propanol are in liquid state at room temperature making it easy not only to storage but also to proceed with the cell refuelling [1, 8].

Energetic density of some alcohols (methanol: 6.09 $kW.h.kg^{-1}$, ethanol: 8.00 $kW.h.kg^{-1}$) are pretty close to the energetic density of fossil fuels (hydrocarbons: 10.00 $kW.h.kg^{-1}$, gasoline: 11.00 $kW.h.kg^{-1}$), for this reason DAFCs present a great potential on the power production devices universe [1].

The oxidation of some alcohols is a slow and complicated reaction where intermediate products are formed. These products stay adsorb onto the anode surface poisoning the active sites of the catalyst. Efforts have been made in order to develop catalysts able to overcome these hurdles [1].

The crossover, whether it is fuel crossover towards the cathode or water crossover towards the anode, is an important issue once it is one of the phenomena that affects directly the performance of these cells [1, 8].

DAFCs are a promising technology for batteries substitution as they can supply electrical power to portable applications for periods of time up to ten times longer than batteries.

Within the DAFCs the devices with a higher level of development are the direct methanol fuel cells (DMFCs). Direct ethanol fuel cells (DEFCs) are a more recent technology that is in first steps of investigation.

2.4. Market

The technology of fuel cells has a very promising competitive potential on the electrical generation market due to some of its features such as modularity, wide power output range among others [8].

Worldwide commercialization of fuel cells, contemplating portable and stationary applications and on the transports sector, grew 214% between 2008 and 2011. Data concerning the number of units sold and associated with the power installed, presented in Figure 2.4, show that in 2012 the sector with the highest volume of sales was the portable applications sector, although, this was not the sector with the highest value of installed power, since this place belongs to the stationary applications [8].

Accounting for the 2012 numbers it can be stated that PEMFCs type were the leaders in both volume of sales and installed power [8].

2013 data forecasts a growth of 104% between 2010 and 2014 which would mean that 1.5 GW had to be installed annually during that period. Perspectives to fuel cell industry, again based on 2013 data, point to transactions reaching up to $19.2 thousand millions by 2020 being the United States of American, Japan, Germany, South Korea and Canada the main countries responsible for the development and commercialization of fuel cells [8].

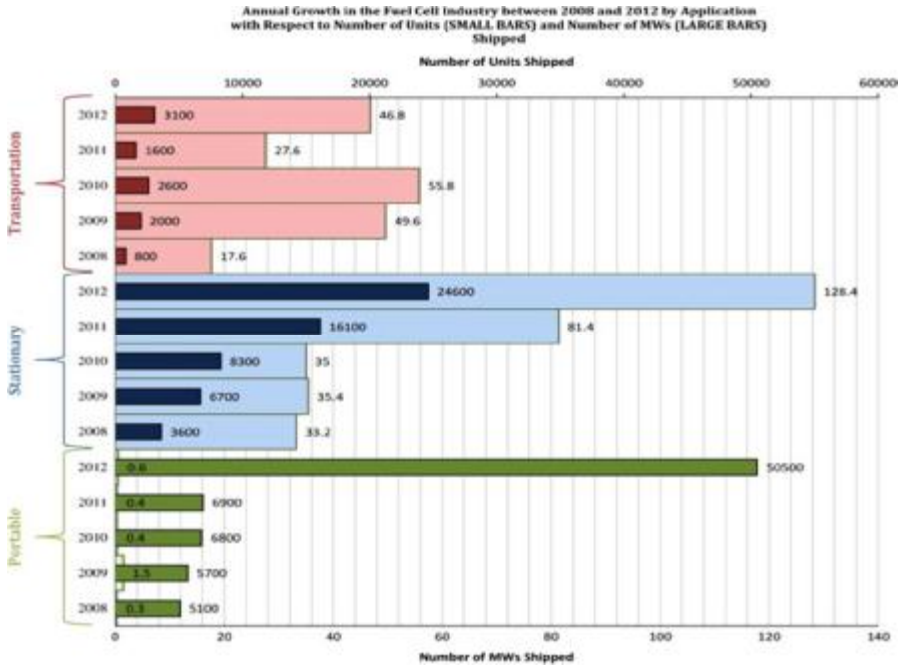

Figure 2.4 : Annual growth of the fuel cell industry between 2008 and 2012 by application [8].

3. Direct Ethanol Fuel Cells (DEFCs)

The recent energy paradigm relies on increasing the electrical efficiency of both production and consumer devices in order to make the best possible use of energy sources and reduce the gas emissions that are harmful to the environment.

Unlike other technologies DEFCs have low gas emission rates thus fulfilling a part of the energy paradigm. With regard to electrical efficiency of these cells, which is around 40%, this is still far from the ideal values. Due to that, the research community continues to study different combinations in order to increase it.

DEFCs are promising to the field of portable applications due to their autonomy periods, much higher than the ones of the technology currently used, and due to their easy refuelling which allows the renovation of power supply in a short period of time.

The research of DAFCs began with DMFCs, which is why this technology is well developed. Among all the alcohols, methanol was the first fuel to be used since it has the simplest alcohol molecule structure and therefore it should have the best oxidation kinetics. However, the phenomenon of the crossover of fuel molecules from the anode to the cathode proved to be a major technical problem decreasing the cell performance. This issue combined with its toxicity and its production from non-renewable sources led researchers to explore the use of new alcohols such as ethanol [10]. Ethanol has non-toxic properties, making it safe to handle, carries a high energy density, can be produced from the fermentation of biomass, known as biofuel, and the crossover rate is lower due to its higher molecular structure [1, 10, 11].

The main factor that leads to a lower power output for DEFCs is the slow reaction kinetics. The oxidation of ethanol molecule is a more complicated process, due to the C-C bond, involving the formation of different intermediate products. These do not always undergo complete oxidation remaining adsorbed on the catalyst decreasing the electrical production. Therefore, it's essential to find the best catalyst for the oxidation reaction.

There are two types of DEFCs that differ in the way that the fuel and oxidant are provided to the cell. When the feeding takes place in a controlled environment, through a system of pumps and fan, the cell is said to be active and usually this is applied to large scale systems. On the other hand when the distribution of the reactants is made by natural phenomena as natural capillary forces, diffusion, convection and evaporation the cell is said to be passive [12].

3.1. Passive Direct Ethanol Fuel Cells

As stated before, passive feed is a fuel distribution method that runs exclusively on natural phenomena such as natural capillary forces, diffusion, convection and evaporation which don't require neither electrical power nor the use of moving parts [12].

Once the objective of this thesis is to optimize a DEFC to be used in portable applications the type of fuel cell addressed was the passive fuel cell. Another important reason lays on the current imposed from the external charge that is much lower on portable application resulting in smaller rates of fuel consumption and producing lower amounts of heat.

The following subchapters were dedicated to the description of the fundamentals of DEFCs regarding the working principle, thermodynamic, electrochemical reactions and DEFC physical components.

3.1.1. Working Principle of DEFCs

DEFCs convert continuously the chemical energy, stored in an aqueous ethanol solution, to electrical power through an electrochemical reaction (releasing some heat along with it) [2].

Anode and cathode compartments are separated by the electrolyte. The physical separation between the sides where reduction and oxidation reaction occur forces electrons to circulate through the external circuit to reach the cathode. While electrons travel through the external circuit, protons will cross the electrolyte to reach the cathode side. At the cathode they will be combined with oxygen, in the reduction reaction, to produce water closing the global reaction. The electrical power is generated through the electrical work done by the flux of electrons [2, 13].

Slow anode kinetics, the ethanol and water crossover, the concentration of the aqueous ethanol solution and the catalysts used are the most important parameters that influence the overall DEFC power production [13].

3.1.2. Physical Components of Passive DEFCs

Passive DEFCs devices consist in a sequence of layers each one with a specific role therefore, depending on the role of each layer they can be made from different materials and have different geometries and structures. The assembly sequence of the layers is: cathode end plate, rubber isolating plate, connector plate, cathode diffusion layer, cathode catalyst layer, membrane, anode catalyst layer, anode diffusion layer, connector plate, isolating rubber plate and the anode end plate (Figure 3.1) [12].

The membrane electrode assembly, MEA, is a set of layers which includes the cathode diffusion layer, the cathode catalyst layer, the electrolyte membrane, the anode catalyst layer and the anode diffusion layer. MEA properties can be modified by changing the features of at least one of its layers, e.g., changing the material or the thickness [1].

There are two types of MEA preparation concerning the support of the catalysts layers. One of the preparation methods is the catalyst-coated membrane (CCM) where the catalysts layers are directly assembled on both sides of the membrane and on the other preparation method the catalysts layers are assembled onto the diffusion layers [1].

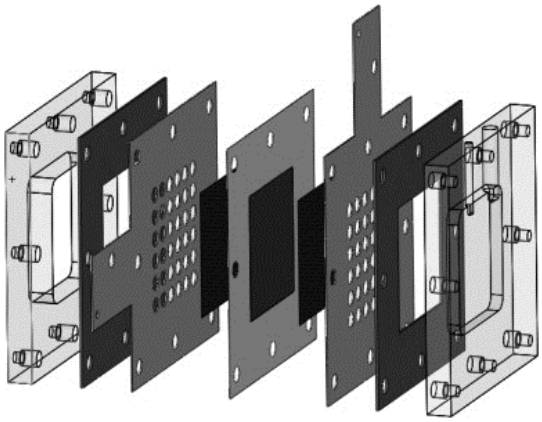

Figure 3.1 : Schematic representation of the DEFC components in the right assembly sequence [12].

The type of the electrolyte membrane usually used in a DEFC is a proton exchange membrane, PEM, made of Nafion. The PEM doesn't just act as the proton carrier but also as the anode and cathode separator [1]. Still, fuel and water molecules are small enough to fit in the Nafion's pores crossing the membrane and reaching the other compartment. The crossover phenomenon leads to fuel loss and to the flooding of the cell decreasing its performance. To reduce the crossover, sometimes it's necessary to use thicker membranes.

Diffusion layers, also known as gas diffusion layers (GDLs), play a very important role regarding the distribution of reactants, the removal of products and also the electronic conduction so, these layers need to be porous and their material should be able to easily transport electrons [13]. Thus, carbon paper (CP), carbon cloth (CC) and ELAT are the materials commonly used.

Two connector plates are placed near to the anode and cathode GDLs to harvest or to supply the electrons to the ongoing electrochemical reaction. These plates can have different geometries and should be made of materials with high conductivity, such as metals, to minimize the electronic transport resistance, e.g., stainless steel or gold plated copper plates.

In order to prevent electrons from escaping the circuit isolating rubber plates are placed on each side of the cell. Finally, to hold together this sandwich-like structure, there are two acrylic end plates. The end plate on the anode side has a reservoir to store the liquid fuel, and the cathode side end plate has a hole to provide the contact between the cathode and the oxygen [12].

3.1.3. DEFCs Thermodynamics

Energy assumes many forms throughout the Universe and as Lavoisier, a French chemist of the 18-century, stated *"Nothing is lost, nothing is created, everything is transformed."*. Thermodynamics is

the study of energy transformation from one form to another predicting the upper limit of the maximum level of energy transformation. To DEFCs Thermodynamics is the key to assess the theoretical values of energy output that can be reached considering an ideal fuel cell [6].

The noblest form of energy is electrical energy because it can be transformed in almost all the other energy forms so the study of new processes of electrical energy production becomes an important issue. DEFCs are fuelled with ethanol which contains stored energy in its chemical structure and in order to release it the bounds of the molecules must be broken in an electrochemical reaction where new smaller molecules and electrons will be formed. The result of the continuous reaction is a flux of electrons with a certain electrical work potential, W_{elec} [6].

Electrical work is related to another thermodynamic potential called Gibbs free energy (G). The best description for Gibbs free energy is that it represents the net energy that has to be transferred from the environment to create the system, it also represents the maximum energy that can be produced by the system. Assuming that over the process both temperature and pressure stay constant the mathematical relationship between the two concepts is expressed by Equation 3.1 where, ΔG is the variation of Gibbs free energy. For a temperature of 25ºC and 1 atm of pressure the value of variation of Gibbs free energy is -1326.7 kJ.mol^{-1} [10].

$$W_{elec} = - \Delta G \tag{3.1}$$

Once determined the value of W_{elec} it is possible to calculate the value of the maximum potential of the cell (E_{cell}), also known as its Nernst potential, using Equation 3.2 where n is the number of moles of electrons transferred and F is the Faraday's constant with the respective values of 12 mol and 96485.34 C.mol^{-1} (Coulomb per mol of electrons) [6].

$$W_{elec} = n.F.E_{cell} \tag{3.2}$$

In the end the maximum potential, also known as open circuit voltage (OCV), of an ideal DEFC is 1.145 V [10]. But in real operation it is necessary to account for the energy losses that occur in the energy transformation process. Thus to know the potential of a real fuel cell several efficiencies must be determined [6].

Even when talking about energy conversion in an ideal scenario it cannot be assumed that the efficiency will be 100% because only a part of the total energy of the system, the useful energy, is available to participate on the energy transformation process. This efficiency is the reversible thermodynamic efficiency of the fuel cell (ε_{thermo}) and it can be determined by Equation 3.3 where ΔH is the enthalpy variation which, to a temperature of 25º C and a pressure of 1 atm, is -1367.9 kJ.mol^{-1}. Under these operating conditions ε_{thermo} is 97% but, there are other efficiencies that have to be considered: the voltage efficiency of the fuel cell ($\varepsilon_{voltage}$) and the fuel utilization efficiency (ε_{fuel}) [10].

$$\varepsilon_{thermo} = \frac{\Delta G}{\Delta H} \tag{3.3}$$

The voltage efficiency represents the irreversible losses due to kinetic effects and is calculated as the ratio between the real operating voltage given by the fuel cell (E) and the maximum voltage predicted by Thermodynamics (E_{cell}), Equation 3.4 [6].

$$\varepsilon_{voltage} = \frac{E}{E_{cell}} \tag{3.4}$$

When fuel is provided to a fuel cell it doesn't mean that every single molecule is going to react as it should, some molecules can participate in side reactions and others can flow through the cell not being consumed so, this efficiency estimates the amount of fuel molecules that follows the right path, Equation 3.5, where i_{cell} is the current produced by the cell and i_{C2H5OH} is the current generated by the ethanol molecules crossover [6].

$$\varepsilon_{fuel} = \frac{i_{cell}}{i_{cell} + i_{C_2H_5OH}} \tag{3.5}$$

The overall efficiency of a real fuel cell (ε_{real}) may be determined combining the three efficiencies as shown in Equation 3.6 [6].

$$\varepsilon_{real} = \varepsilon_{thermo} \times \varepsilon_{voltage} \times \varepsilon_{fuel} \tag{3.6}$$

3.1.4. Electrochemical Reactions of DEFCs

The electrochemical reactions of DEFCs are the ethanol oxidation, at the anode, Equation 3.7, and the oxygen reduction, at the cathode, Equation 3.8, which combine in a global reaction, Equation 3.9. Figure 3.2 is a scheme that shows the path covered by the different elements of the electrochemical reaction.

$$CH_3CH_2OH + 3H_2O \rightarrow 2CO_2 + 12H^+ + 12e^- \tag{3.7}$$

$$3O_2 + 12H^+ + 12e^- \rightarrow 6H_2O \tag{3.8}$$

$$CH_3CH_2OH + 3O_2 \rightarrow 2CO_2 + 3H_2O \tag{3.9}$$

While the reduction of oxygen occurs without no apparent issues the oxidation of ethanol has a sluggish kinetic and it's a complex reaction that forms intermediate species, the acetic acid and the acetaldehyde, due to the cleavage of ethanol's C-C bond [10, 14].

Equation 3.7 represents the complete oxidation of ethanol which involves the release of 12 electrons but since this reaction it's almost never carried out until the end the number of electrons actually released can be between 3 and 4 [15].

The kinetics of the oxidation reaction depends on the temperature, catalyst, ethanol concentration, pressure and on the physical state of the reactants. When the temperature is high, over 100º C, kinetics tends to be fast but, at room temperature, around 20 and 25º C, kinetics is not favoured [1].

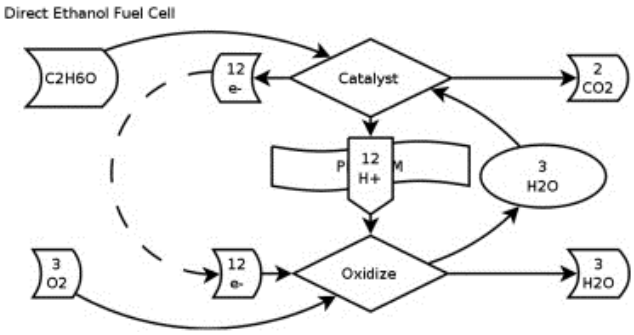

Figure 3.2: Reaction flowchart of direct ethanol fuel cell [1].

Since anode's kinetics depends on the fuel concentration, higher fuel concentrations should have higher performances. However, the crossover of fuel molecules to the cathode side also increases. This results on a fuel loss and, at the cathode side, on the competition of ethanol and oxygen for the catalyst active sites, decreasing the fuel cell performance.

For that matter the next paragraphs are dedicated to the understanding how catalysts work and what difference does it make when a new metallic element is added to a carbon supported Pt-based catalyst.

Catalysts are used to lower the activation energy of the reaction to facilitate it, catalysts are able to do that by providing specific sites for the reaction to take place called active sites.

A carbon supported Pt catalyst promotes the adsorption and decomposition of ethanol, Equations 3.10 and 3.11, however the intermediate species that are formed as well as some of the ethanol molecules stay strongly adsorbed on the active sites resulting on the rapidly poisoning of Pt [16, 17]. Therefore, researchers have tried to mix Pt with another metal, a cocatalyst, obtaining better results. *Antolini et al.* [16] explained the good results of the binary catalysts based on the bifunctional effect and on the intrinsic mechanism.

$$CH_3CH_2OH \rightarrow [CH_3CH_2OH]_{ad} \rightarrow C1_{ad}\ , C2_{ad} \rightarrow CO_2 \text{ (total oxidation)} \quad (3.10)$$

$$CH_3CH_2OH \rightarrow [CH_3CH_2OH]_{ad} \rightarrow CH_3CHOH \rightarrow CH_3COOH \text{ (partial oxidation)} \quad (3.11)$$

Bifunctional effect also known as promoted mechanism occurs when next to the Pt active sites are the cocatalyst sites which will accommodate the dissociative adsorption reaction of water providing the oxygen-containing species to ethanol oxidation reaction leading to the oxidation of some of the intermediate products and improving the cell's efficiency [16, 18].

The intrinsic mechanism is related to the electronic interactions between Pt and cocatalyst metal, e.g. Ru, Sn, W, Rh, Re, Mo, Ti or Ce. The presence of the cocatalyst modifies the electronic structure of Pt changing the mechanism of adsorption of oxygen-containing species [16].

The main purpose of the present work was to improve anode's kinetics using different anode catalysts with different compositions. Based on that, this work focuses on the studying the binary (Pt-Sn) and ternary (Pt-Sn-based) catalysts testing for each combination different metal proportions.

3.2. State of the Art

DEFCs have been studied, in the last years, in order to improve their performance, by testing different structural and operational combinations, towards their commercialization.

Among all the DEFC's components the anode catalyst is the one who has been more investigated since the fuel oxidation reaction, one of the most important drawbacks of this technology, depends on its composition and structure [19]. Based on that, the following sub-section will address a brief status report on the work done on this field.

Studies using carbon supported Pt catalysts shown that although Pt alone was the most active metal for the ethanol oxidation it wasn´t the best catalyst because it adsorbed permanently some ethanol molecules and its surface was also easily poisoned by CO species. So, in order to overcome this problem, *Antolini et al.* [16] used a common catalyst for DMFC, Pt-Ru carbon supported, but, as *Kamarudin et al.* [1] also reported, this binary catalyst turned not to be a good solution [1, 13, 16].. *Vigier et al.* [14] reported an increase of DEFC's performance with the addition of Sn and *Antolini et al.* [16] supported these results with a thorough study of the phenomenon. Within the carbon supported bimetallic catalysts tested, such as Pt-W, Pt-Rh, Pt-Pd, Pt-Re among others, the Pt-Sn catalyst was the one who shown better results [16] *Song et al.* [13] proposed the mechanism of the ethanol oxidation reaction for the Pt-Sn catalyst, Figure 3.3, which led to the conclusion that Sn doesn't help in the C-C bond cleavage but instead it provides adsorbed OH species to promote the early stages of the oxidation process [13, 18].

At this point in the DEFC's research, in spite all the efforts made to reach better performances, this technology is still far behind when compared to DMFCs. The solution to obtain better results is to achieve the complete oxidation of ethanol therefore, it's necessary to break its C-C bond. *Antolini et al.* [16] suggested that the C-C bond cleavage could be accomplished by adding a third metal to de Pt-Sn catalyst. The addition of a third metal, to form a ternary catalyst, also provided an increase on the dehydrogenation activity and on the cleavage of C-O improving the oxidation process. Pt-Sn-based catalysts most studied combinations use, as the third element, Ru, Sn, Ni, Co, Ir, Pd or Rh [1, 16, 18, 20].

Antolini et al. [16] studied Pt-Sn-Ru carbon supported catalyst with different metal proportions and found that the one with lower amounts of Ru performed better. This happened because lower Ru

contents allowed the interaction between Sn and Ru oxides increasing the activity of the ternary catalyst which did not happened with high Ru contents [16].

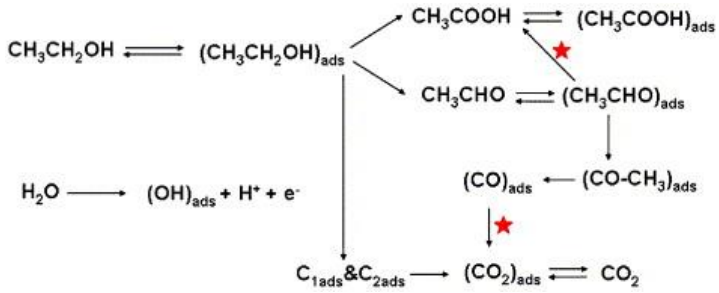

Figure 3.3 : The schematic representation of ethanol electrooxidation over Pt-Sn catalysts [13].

Other Pt-Sn-based combinations were tested by *Beyhan et al.* [20] namely Pt-Sn-Ni, Pt-Sn-Co, Pt-Sn-Rh and Pt-Sn-Pd with a nominal composition of (80:10:10) [at%]. Their results shown a significant improvement in the overall catalyst performance when Ni or Co were added as the third metal. Comparing the results of the Pt-Sn-Ni, the Pt-Sn-Co and the Pt-Sn catalysts *Beyhan et al.* [20] concluded that the presence of Ni or Co made a major difference in the activity of the catalyst surpassing the Pt-Sn catalyst performance because, the presence of theses metals helps to strengthen the bond between the Pt and the carbon support therefore, improving the stability of the catalyst [20].

Fatih et al. [21] studied a more complex catalyst with four metallic elements (Pt-Ru-Ir-Sn), this quaternary catalyst proved to be once more better than the Pt-Sn-Ru and Pt-Sn catalysts[21][21][21]

3.3. Advantages and Disadvantages of Passive DEFCs

DEFCs have some of the DMFCs advantages as well as some of their disadvantages for example, the use of a liquid fuel, because it is liquid it's easy to handle and storage thus favouring the refuelling process. Their silent operation, modular structure and great autonomy are other features also shared by both DAFCs [11].

Ethanol can be produced from renewable sources, biomass, and its energy density is high and comparable to those of some of the fossil fuels. In terms of toxicity, ethanol is harmless to the environment therefore, it is not necessary to adopt tight security measures [1, 8, 9, 11].

During the power production process the reactions of reduction and oxidation generate water a very small amounts of CO_2 and some intermediate products that have no impact on the environment making the DEFCs an almost clean technology.

Operating costs are low because ethanol is relatively cheap and the oxygen is provided by the air but, the production costs are, on the contrary, very high since this technology is still at an early stage of development and uses noble metals as catalysts which are very expensive.

Another great advantage of DEFCs is that the fuel crossover rate is smaller, compared with DMFCs, due to the higher size of its molecule. Still, the amount of fuel that crosses the membrane to

the cathode side is oxidized on the wrong side of the cell and, at the same time, will force oxygen molecules to compete for the cathode active sites [1, 10, 19].

If on one hand, higher molecules are an advantage for lowering the crossover rate on the other hand, they are also tougher to oxidize because of their complex mechanism of reaction. This means that this reaction has slow kinetics and is more likely to stay incomplete [1].

In ethanol case the complexity of the reaction comes from the cleavage of the C-C bond which leads to the formation of intermediate products, acetic acid and the acetaldehyde, that can poison the catalyst surface [19].

All of these issues contribute to poor fuel cell performances and so they must be overcome in order to potentiate the launch of this technology on the market.

3.4. Applications for Passive DEFCs

Passive DEFCs are very promising as backup and remote power systems and as portable power sources, becoming an alternative to conventional batteries or power generators [22].

Nowadays there are very few DEFC devices being commercialized since the majority of these devices are small scale systems and most of them developed in laboratory scale. Therefore, there aren't many DEFCs in the prototype phase [22].

Two of the DEFC devices currently being commercialized are the Bio-energy Discovery Kit and the EOS Direct Ethanol Fuel Cell. Bio-energy Discovery Kit, Figure 3.4, it's a Horizon Fuel Cell product suited to educational purposes and works with a mixture of vodka and water, as the fuel, and with air.

Figure 3.4: On the right side the EOS Direct Ethanol Fuel Cell on the left side the Bio-energy Discovery Kit [1].

The EOS Direct Fuel Cell, Figure 3.4, developed by NDC Power, is a portable charger to small electronic devices such as laptops and mobile phones, it uses a non-platinum catalyst, is able to provide power in a range of 3-250 W, has a lifetime operation of 3700 hours and doesn't require catalyst regeneration [1, 22].

NDC Power is also developing a prototype, the EOS 1 kW Direct Ethanol Fuel Cell, that consists in a 36 fuel cell stack with 1200 hours of lifetime operation [22].

In 2007 a team from Offerburg University participated in a competition with a vehicle supplied by DEFCs and won the third place. This vehicle had a stack of 60 cells and was able to produce 40 V with a maximum power of 2 kW allowing the vehicle to run at 2716 km/L [1, 22].

In spite of all the efforts made on the development of DEFCs throughout the years, the truth is that their mass production and commercialization remain in a faraway future.

3.5. Summary

Over the current chapter all the important information about direct ethanol fuel cells is summed up to give the reader the fundamental knowledge about this thesis theme.

Therefore, in Chapter 3 can be found the DEFCs working principle, physical components, electrochemical reactions, as well as, the thermodynamics of the process. It is, also, provided the overall perspective concerning the obstacles of this technology, the work that has been performed on the catalysts field and also the areas where DEFCs can be integrated.

This technology is still being developed and so, it still needs to overcome some hurdles such as the incomplete oxidation reaction and its sluggish kinetics, as well as, the fuel crossover to the cathode side not only because it represents the loss of fuel but also because it creates competition, between oxygen and ethanol, for the cathode active sites. The combination of these two issues leads to a major loss on the fuel cell performance.

In order to overcome these obstacles researchers are currently studying new anode catalysts, either binary or ternary catalysts, testing new gas diffusions layers and membranes.

4. Experimental Set Up

As mentioned before, further DEFC development is crucial to turn these cells into a commercial product therefore, this chapter is dedicated to the description of all the important information related to the experimental work, such as the operating conditions, the equipment used and the components of the cell. The experimental procedure followed during the tests is also described in a simplified way.

4.1. Design of the Passive DEFC

The passive DEFC is a device composed by several elements in a sandwich arrangement hold together by a set of 8 screws (Figure 4.1) in the following order: cathode end plate, rubber plate, connector plate, cathode diffusion layer, cathode catalyst layer, membrane, anode catalyst layer, anode diffusion layer, connector plate, rubber plate and the anode end plate.

The specific set of elements used in this experimental work is described in detail bellow and can be found on Tables 4.1 and 4.2, and in Figure 4.2.

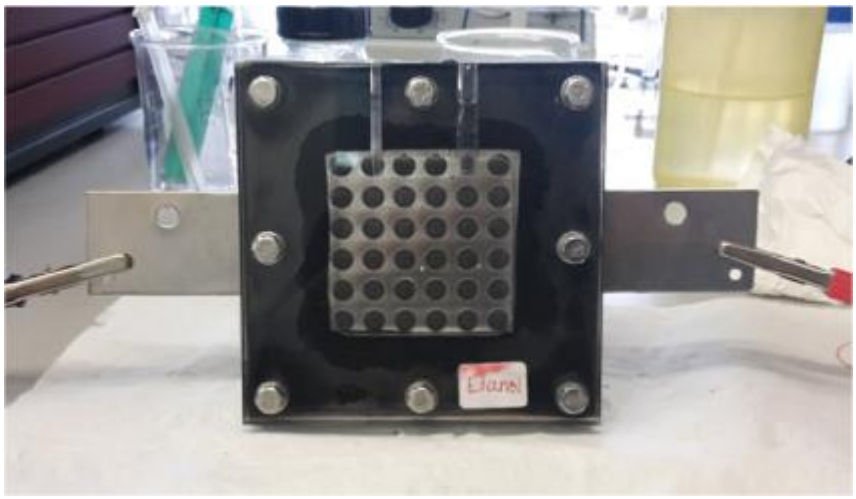

Figure 4.1: Passive DEFC used to perform the tests.

- Membrane Electrode Assembly (MEA): this element comprises three components the electrolyte membrane, the gas diffusion layers (GDLs) and the catalysts.
  - Ø Electrolyte membrane: the membrane used was a PEM type membrane made of Nafion 117;
  - Ø Gas Diffusion Layers (GDLs): it was used two types of GDLs, made of different carbon support materials, such as carbon paper and carbon cloth. These materials differ in terms of porosity due to the different types of fibres and fibre's distribution conferring a more porous structure to carbon cloth;

    On this experimental study the GDLs were used as the backing layer of the catalysts. On the anode it was used carbon paper and cloth and on the cathode it was used carbon paper with two different thicknesses;

Table 4.1 : Specifications of the passive DEFC components.

Total area of the cell		100 cm^2					
Active area of the cell		10.2 cm^2					
Component	Material	Dimensions (cm x cm x mm)	Reference	Load	PTFE	MPL	Supplier
End Plates	Acrylic	10 x 10 x 10	------	------	------	------	------
Isolating Plates	Rubber	10 x 10 x 1	------	------	------	------	------
Connector Plates	316 Stainless Steel	10 x 10 x 0.5	------	------	------	------	------
Membrane	Nafion 117	10 x 10 x 0.183	------	------	------	------	QuinTech
Cathode Gas Diffusion Layer / Catalyst	Carbon Paper	5 x 5 x 0.400	BC-H25-10S	1.0 Pt mg/cm^2	Yes	Yes	
		5 x 5 x 0.400	BC-H25-05S	0.5 Pt mg/cm^2	Yes	Yes	
		5 x 5 x 0.270	BC-H25-05F	0.5 Pt mg/cm^2	Yes	Yes	
Anode Gas Diffusion Layer	Carbon Cloth	5 x 5 x 0.400	CC-G-7	------	No	No	
		5 x 5 x 0.425	CC-G-8		No	No	
	Carbon Paper	5 x 5 x 0.110	EC-TP1-030T		Yes	No	
		5 x 5 x 0.190	EC-TP1-060T		Yes	No	

- **Ø** Catalysts: the catalysts used on the cathode were commercial products supplied by QuinTech (Table 4.1) and the anode catalysts were prepared and placed on the GDLs by the Laboratory of Catalysis and Materials (LCM) at the Faculty of Engineering, University of Porto (Table 4.2).

  The catalysts preparation process started with the use of Carbon Black Printex 200 as support. Then, the monometallic Pt/CB catalyst was prepared by incipient wetness impregnation with an aqueous solution of H_2PtCl_6 (Alfa Aesar), with a content of noble metal, for each catalyst, listed on Table 4.2. The bimetallic Pt-Sn/CB catalysts were prepared by incipient wetness co-impregnation with aqueous solutions of H_2PtCl_6 (Alfa Aesar) and $SnCl_2 \cdot 2H_2O$ (Sigma Aldrich) with the appropriate concentration to achieve a Pt content of X wt.% and X wt.% of Sn. The metal proportions and combinations used were based on *Kamarudin et al.* [1], *Beyhan et al.* [20] and *Cunha et al.* [11]. After impregnation, the samples were dried at 100 ºC for 24 h. Then, the samples were calcined under nitrogen flow at 200 ºC for 1 h and reduced at 200 ºC under hydrogen flow for 3 h. Once the preparation of the catalyst was finished the next step was to place it on the GDL to achieve that, a certain amount of catalyst was weight, according to the loading specifications, mixed with 1 mL of Ethanol Absolute PA and 100 µL of Nafion and left for 1 hour in an ultrasonic bath to disperse the solution. Then, with the help of an airbrush the catalyst was sprayed on one side of the GDL;

- Connector plates: these plates were made of stainless steel and each one had 36 circular holes, with 6 mm diameter making a total area of 10.2 cm^2. These holes were drilled to allow the reactants to pass through a reach the catalyst layer and to remove the products.

Therefore it was assumed an active area of 10.2 cm^2 despite the fact that the catalyst had an active area of 25 cm^2.

- Isolating plates: to avoid the contact between the connector plates and end plates, isolating rubber plates were placed between these two layers;
- End plates: these plates offer structure, support and protection to the other elements of the cell. On both anode and cathode side the plates were made of acrylic with 10 x 10 cm. However, each plate had a specific design in other to be able to provide the reactants so, on the cathode side the plate had a 5 x 5 cm square hole, and on the anode side the plate had a 12.5 cm^3 reservoir to feed the ethanol.

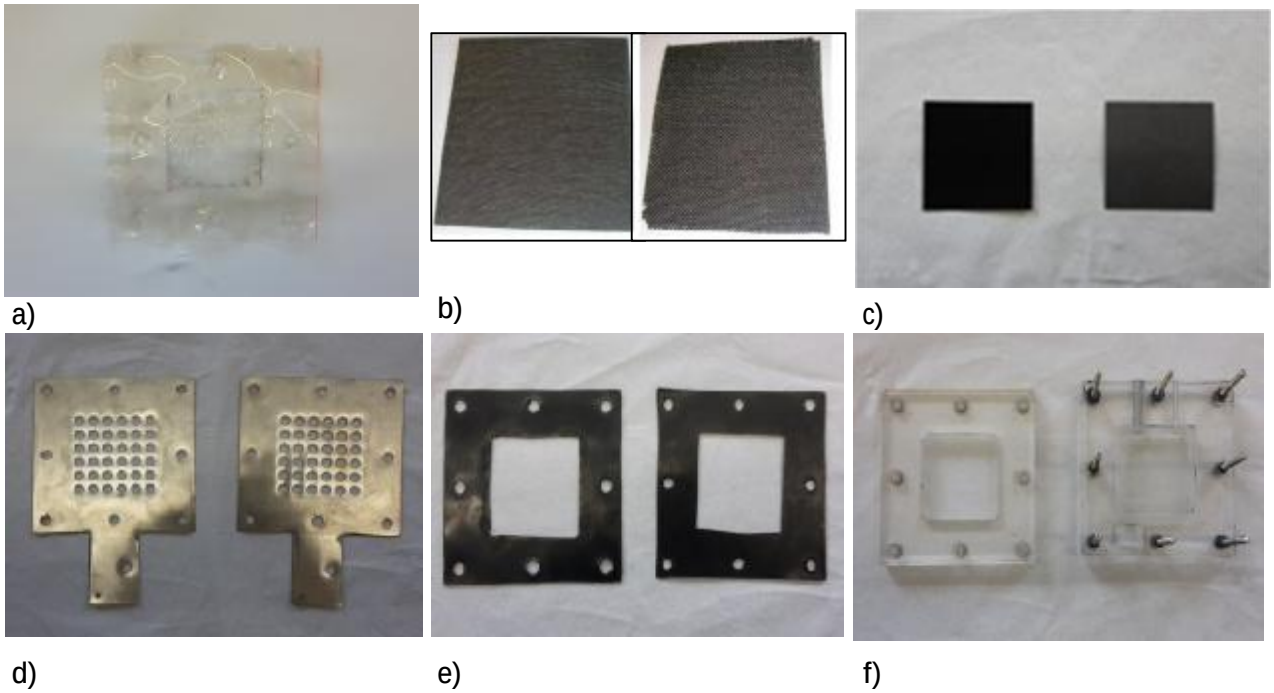

Figure 4.2: Set of elements used on the passive DEFC: a) Nafion 117 proton exchange membrane; b) on the left carbon paper, on the right carbon cloth; c) catalyst layer; d) stainless steel connector plates; e) on the left cathode end plate and on the right the anode end plate.

Table 4.2 : Different catalysts and GDLs tested.

Catalyst			Gas Diffusion Layer			
Composition		Load (mg/cm^2)	Carbon Paper		Carbon Cloth	
Metal (wt%)	Carbon Black (CB)		Thinner (EC-TP1-030T)	Normal (EC-TP1-060T)	Normal (CC-G-7)	Thicker (CC-G-8)
40% Pt-40% Sn	20%	2		X	X	
		3	X	X	X	X
20% Pt-20% Sn	60%			X	X	
60% Pt-40% Sn (*)				X		
60% Pt-30% Sn-10% Ni (*)				X		
60% Pt-30% Sn-10% Co (*)				X		

(*) these metal percentages correspond to an overall metal percentage of 40%.

4.2. Equipment Used and Operating Conditions

The tests conducted on the passive DEFC were performed with a commercial electrochemical impedance test station, Zahner-Elektrik GmbH & Co. kG, using Thales USB software, in galvanostatic mode which means that the imposed parameter was the current and the measured parameter was the respective voltage, Figure 4.3. With this information it was possible to trace the polarization and power density curves that determine the performance of the fuel cell.

Operating conditions to which the cell was subjected were atmospheric pressure and room temperature.

Generally it was tested three different concentrations, 1, 2 and 3 M, starting with the smaller one and increasing the concentration until the performance of the cell was worse than the previous one.

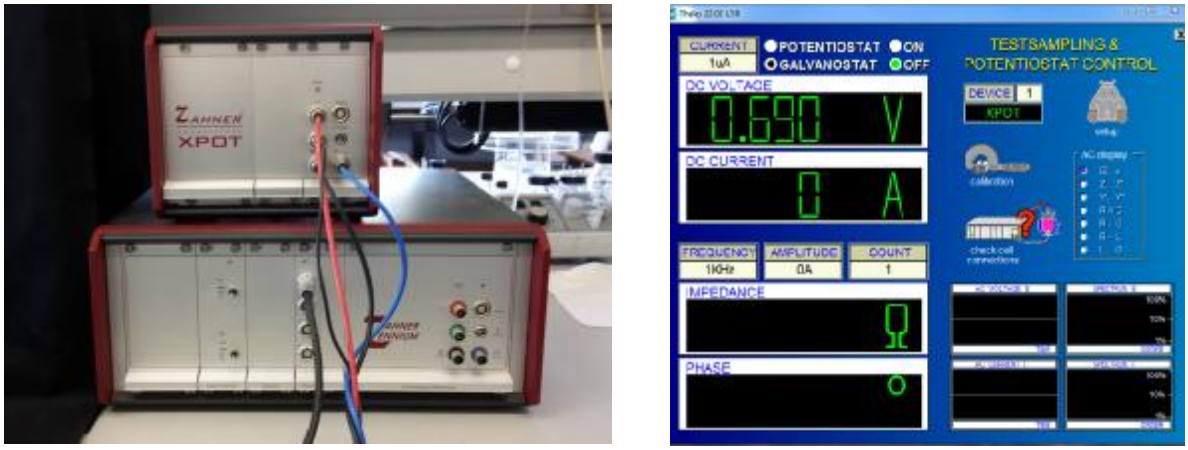

Figure 4.3 : On the left the Zhaner station and Zahner XPOT module and on the right the Thales USB software.

4.3. Experimental Procedure

The procedure followed was:

1. Introduction of the ethanol aqueous solution into the cell's reservoir;
2. Turn on the computer;
3. Turn on the Zhaner station and Zahner XPOT module;
4. Put Zahner XPOT module on the mode "go";
5. Open Thales USB software, chose I/E mode and select "potentiostat control" and then chose the "galvanostat mode";
6. The cell was left to stabilize on the open circuit voltage for at least 15 minutes;
7. On Thales USB software press "on" to start the test;
8. Current was increased in intervals of 0.005 A or 0.010 A every 3 minutes until the voltage reached values under 0.100 V;

9. Once the voltage reached values under 0.100 V press “off” on the software and put Zahner XPOT module on the mode “stop” to terminate the test;
10. Shut down the software and both Zhaner station modules;
11. Remove the ethanol solution from cell’s reservoir replacing it with distilled water;
12. After letting the cell rest for 10 minutes the procedure can be restart.

Note: In order to validate data for each condition tested it was admitted a relative error of 10% between two tests.

5. Experimental Results and Discussion

The experimental results presented in this chapter were obtained following the experimental procedure, using the equipment and operating conditions described in the previous chapter and will be presented below in the form of two curves: curve a) the polarization curve and curve b) the power density curve.

In order to validate the experimental data, for each combination tested, it was admitted an error of 10% between two tests and so, the average of the results of the voltage was used to calculate the power density values. The polarization and power density curves were build using these average values which presented on Appendix (Appendix B to J).

The cell used to perform the tests had an active area of 10.2 cm^2 and the only cell components that were common to all the tests were the PEM, made of Nafion 117, and the connector plates, made of stainless steel.

In this experimental study the design parameters analysed were the cathode thickness, the cathode catalyst loading, the anode catalyst metals, the anode catalyst loading, the anode catalyst metal percentage, the anode GDL material and the operating parameter studied was the ethanol concentration.

5.1. Effect of ethanol concentration

Ethanol concentration is the parameter that determines the maximum power density that the fuel cell can achieve therefore, theoretically the use of higher ethanol concentrations would represent higher values of power density. But, this is not entirely true since the crossover, which represents the loss of fuel, is more significant with the increase of the ethanol concentration. The solution to this problem could be the use of less concentrated ethanol solutions nevertheless, this situation is also not ideal because the use of diluted solutions leads to water crossover problems, which decreases the fuel performance. So, the key to solve these critical issues is to find a concentration that has the lowest impact on the compromise between the concentration of ethanol and the loss of performance.

To assess the effect of ethanol concentration different concentrations with two fuel different cell configurations, which differ on the material of the anode diffusion layer, carbon cloth (CC) and carbon paper (CP), were tested.

Using CC as anode GDL three of the four concentrations tested, 2, 3 and 4 M, obtained similar results however, the 3 M solution was the one who reached the highest values of power density, Figure 5.1.1 .

For the CP as anode GDL, Figure 5.1.2, two of the concentrations tested had very close results even so, the best results were achieved for the 2 M concentration.

Analysing the results for the best concentration with the two different materials it can be observed that even if the best concentration for the CP was smaller than the one for the CC, the configuration with the CP was able to operate to higher values of current density which is an important aspect when taking into consideration future applications of these technology.

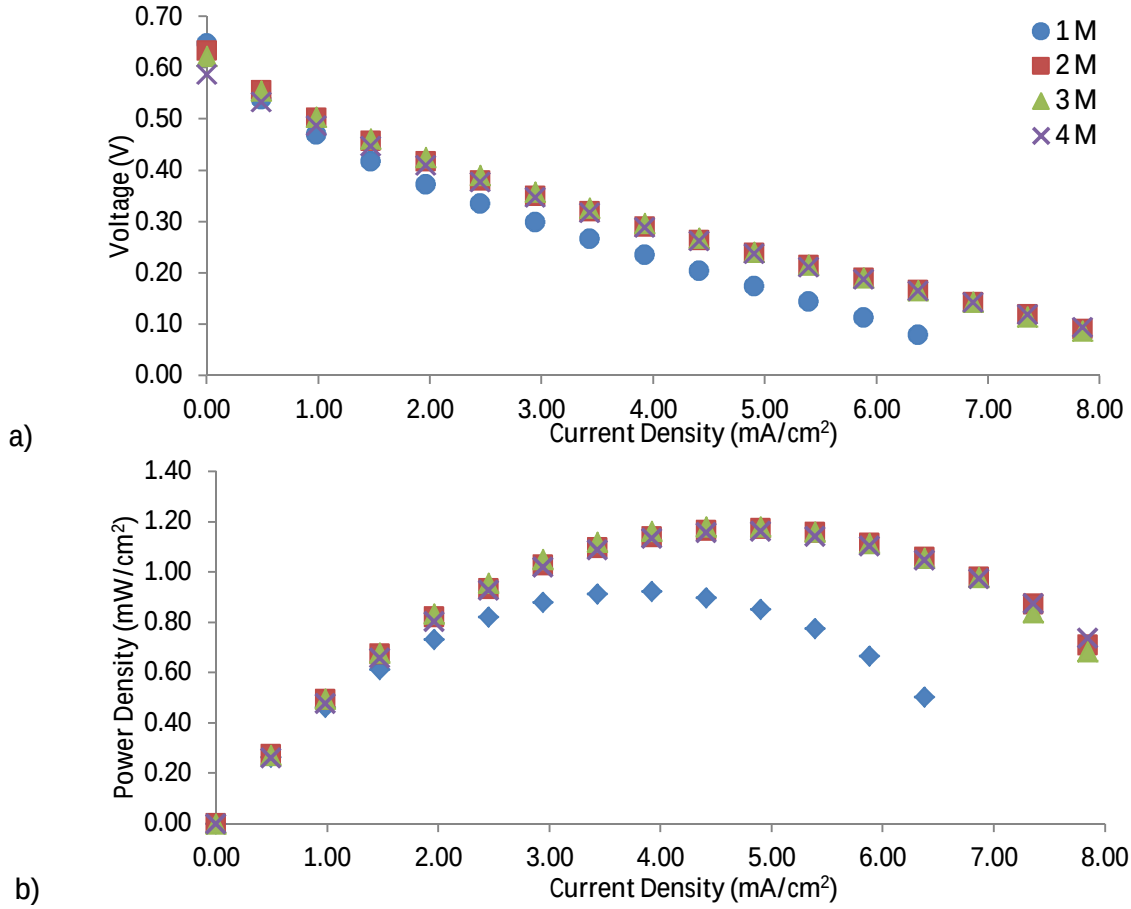

Figure 5.1.1: a) polarization curve and b) power density curve for the effect of ethanol concentration. Design parameters of the DEFC: anode catalyst – 2 mg/cm^2 of 40% Pt - 40% Sn/20% CB in 0.400 mm carbon cloth; cathode catalyst – 1.0 mg/cm^2 of Pt in 0.400 mm carbon paper.

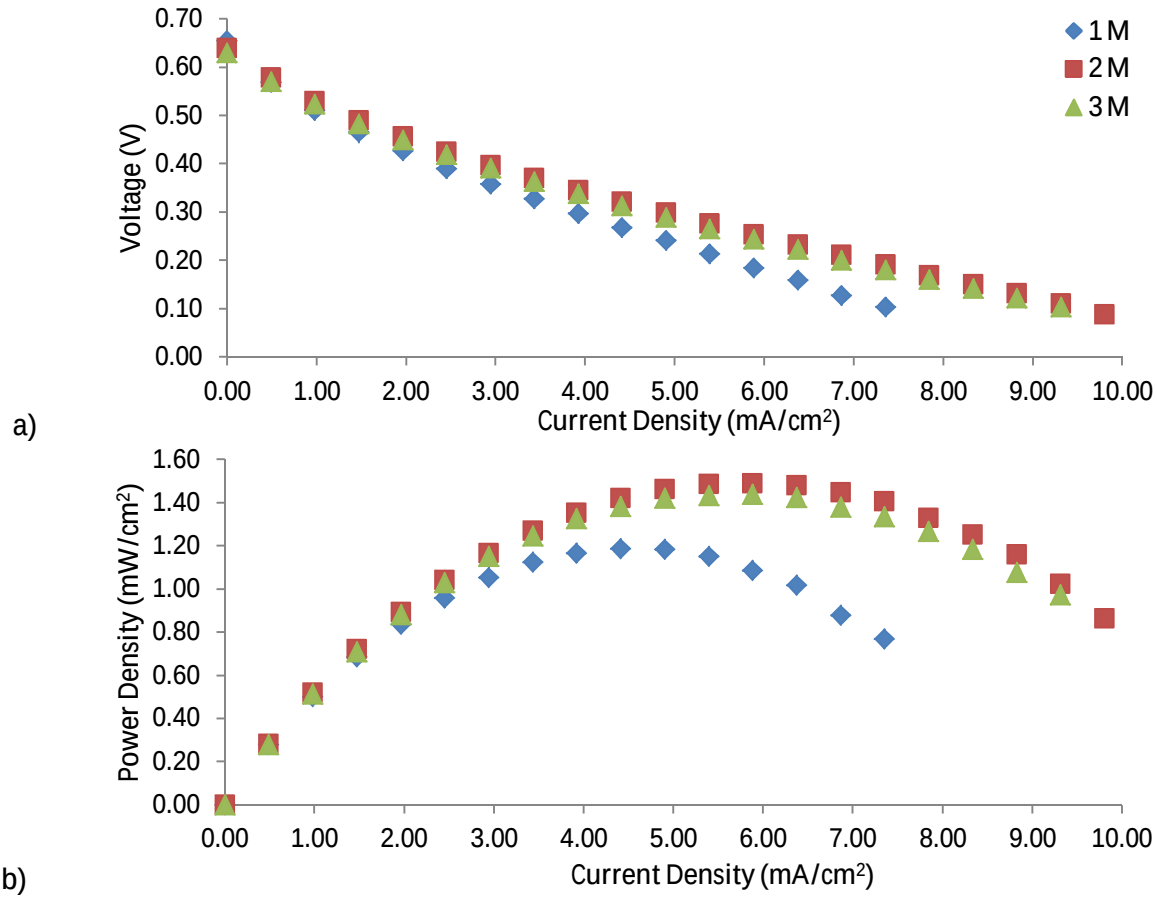

Figure 5.1.2: a) polarization curve and b) power density curve for the effect of ethanol concentration. Design parameters of the DEFC: anode catalyst – 2 mg/cm^2 of 40% Pt - 40% Sn/20% CB in 0.190 mm carbon paper; cathode catalyst – 1.0 mg/cm^2 of Pt in 0.400 mm carbon paper.

5.2. Effect of cathode gas diffusion layer thickness

The reduction reaction of oxygen takes place on the cathode side of the fuel cell and can also be objective of improvement thus, some of its features were studied.

First, it was studied the influence of the cathode GDL thickness and for that it was tested two different thicknesses of the CP, 0.400 mm and 0.270 mm, while maintaining the other components of the cell.

The results obtained using the CC as the anode GDL, Figure 5.2.1, show that the thicker cathode layer, for an ethanol concentration of 2 M, performed better. Analysing the results obtained using CP as anode GDL, Figure 5.2.2, the thicker cathode was once more the one with the best performance but, this time for an ethanol concentration of 3 M.

The performance of the cathode catalyst depends on the diffusion of the oxygen through the GDL and so, it was expected that thinner GDLs would achieve the best results since the mass transport resistance is low which facilitates the oxygen diffusion. However, the water removal from the cathode is also facilitated so, less water goes by back-diffusion towards the anode side, when working with high ethanol concentrations a higher water back-diffusion rate is desirable to supply to the anode the

amount of water needed to the ethanol oxidation reaction therefore, higher performances are achieved in this conditions.

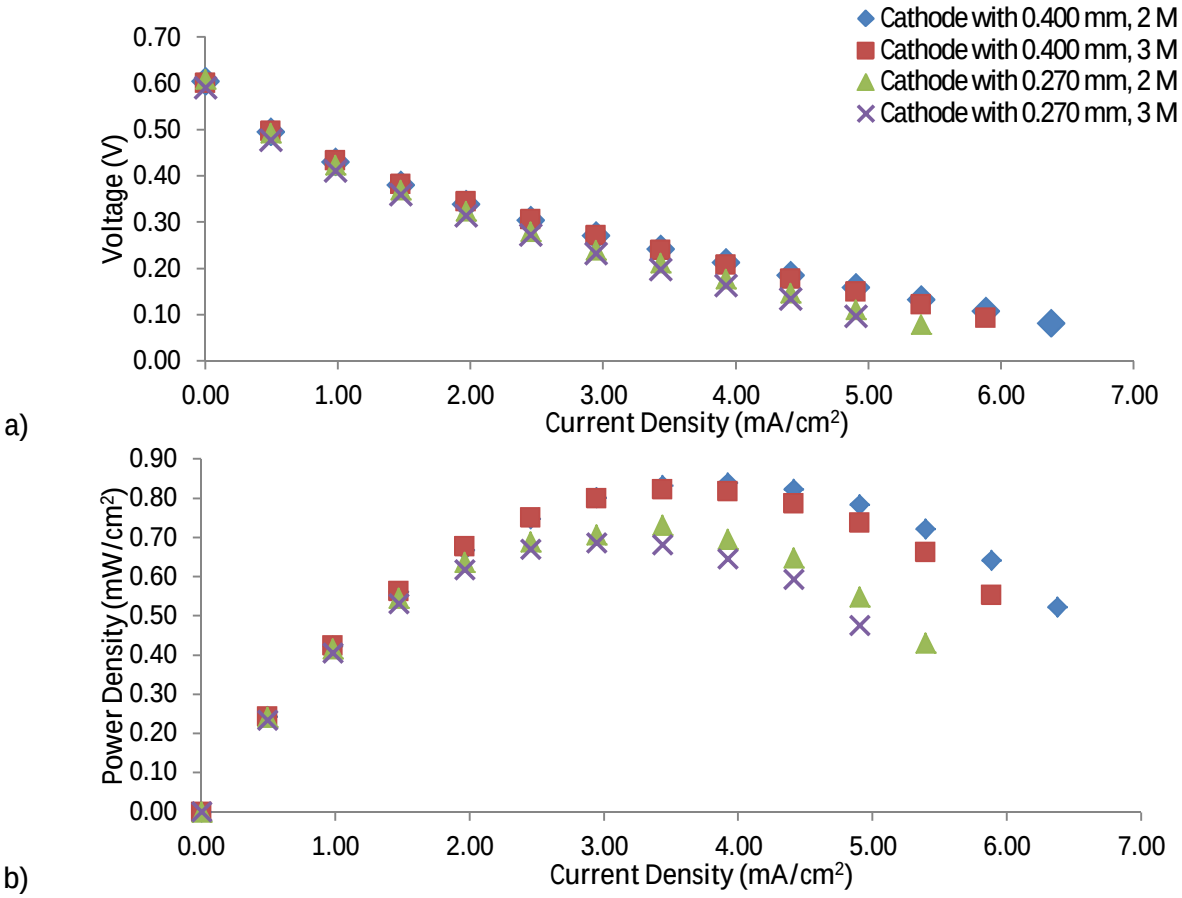

Figure 5.2.1: a) polarization curve and b) power density curve for the effect of cathode thickness. Design parameters of the DEFC: anode catalyst – 2 mg/cm^2 of 40% Pt - 40% Sn/20% CB in 0.400 mm carbon cloth; cathode catalyst – 0.5 mg/cm^2 of Pt in carbon paper.

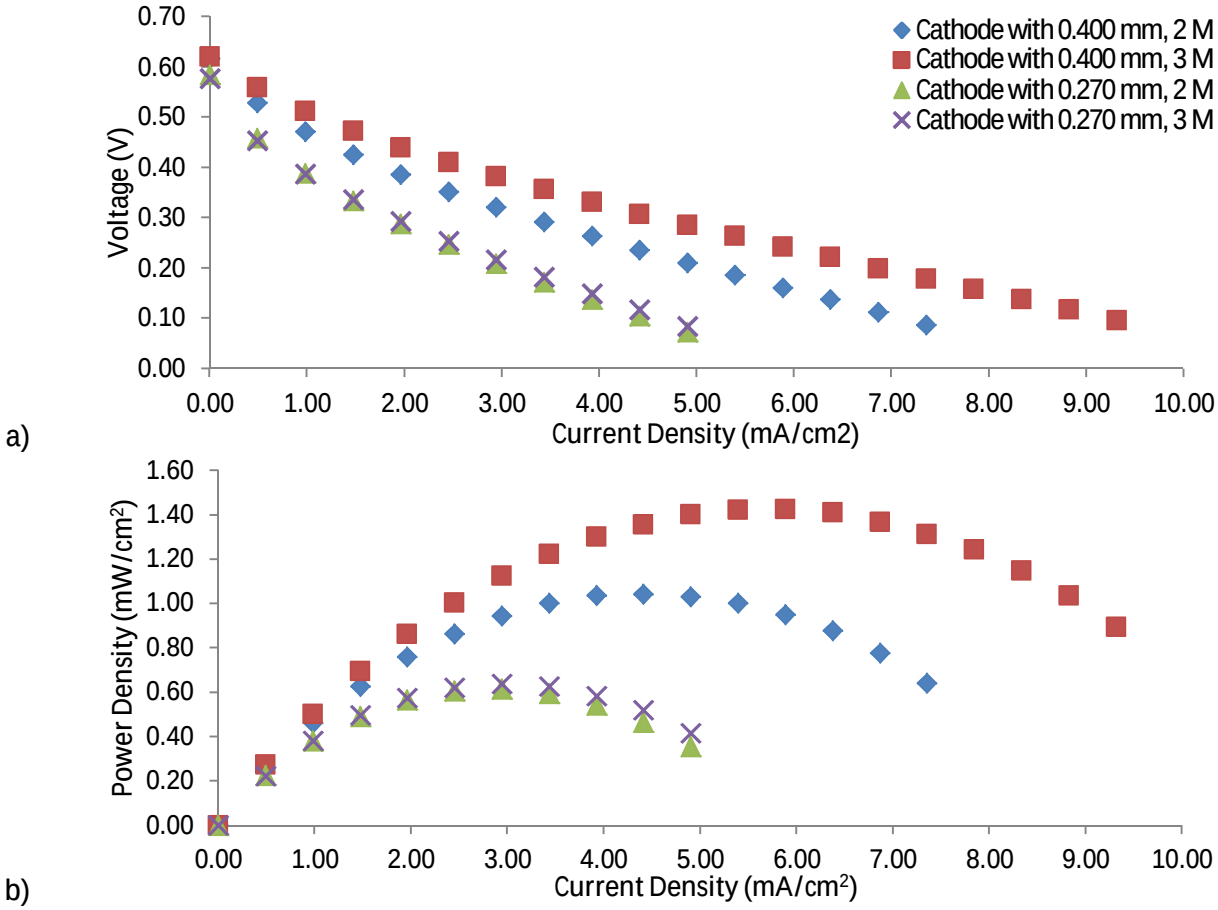

Figure 5.2.2: a) polarization curve and b) power density curve for the effect of cathode thickness. Design parameters of the DEFC: anode catalyst – 2 mg/cm^2 of 40% Pt - 40% Sn/20% CB in 0.190 mm carbon paper; cathode catalyst – 0.5 mg/cm^2 of Pt in carbon paper.

5.3. Effect of cathode catalyst loading

Since Platinum is a very expensive element and represents a significant part of the production costs, it is very important to reduce the amount of Pt that is used. Taking into account that the cathode catalyst is essentially composed of Pt and CB the cathode catalyst loading was studied in order to assess the impact of decreasing the Pt content on the fuel cell performance.

Since, higher loads of catalyst represent a higher number of active sites per square centimetre, which promotes the oxygen reduction reaction, it was expected that the highest cathode catalyst loading would be better. Another important aspect is that the activation energy loss will decrease and can balance some of the energy losses due to the ethanol crossover.

For the tests that had the CC as the anode GDL, Figure 5.3.1, the best results were achieved for the higher cathode catalyst loading, 1 mg/cm^2, and were very similar using 2 M and 3 M solutions.

The results obtained for the CP as anode GDL, Figure 5.3.2, are very interesting since the results for the 3 M ethanol solution and a loading of 0.5 mg/cm^2 the cell was able to reach the same power density values reached in the other tests performed using the higher loading therefore, it is possible to achieve higher performances with a lower catalyst loading.

From this point forward, the cathode catalyst used was the one with the highest loading, 1 mg/cm^2, since it was the one who showed better performances for both tests.

a)

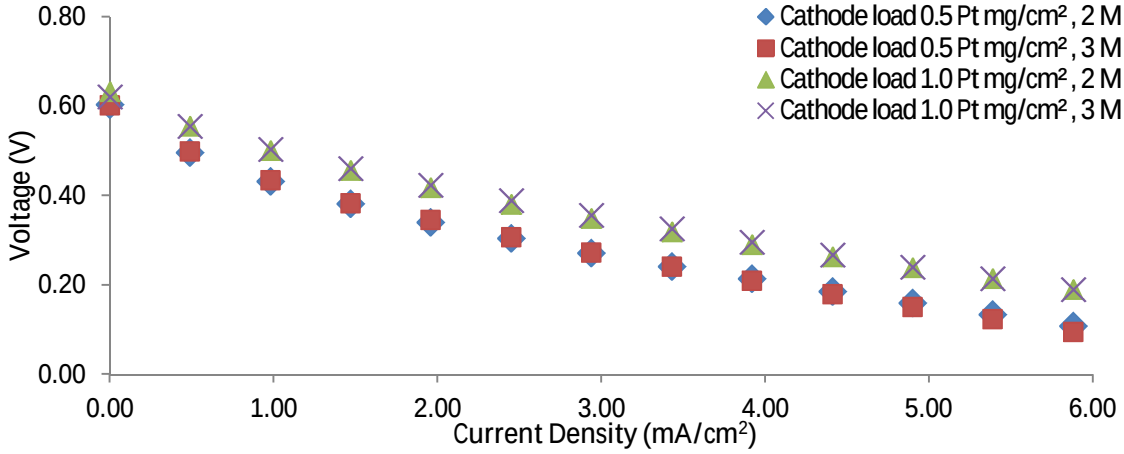

b)

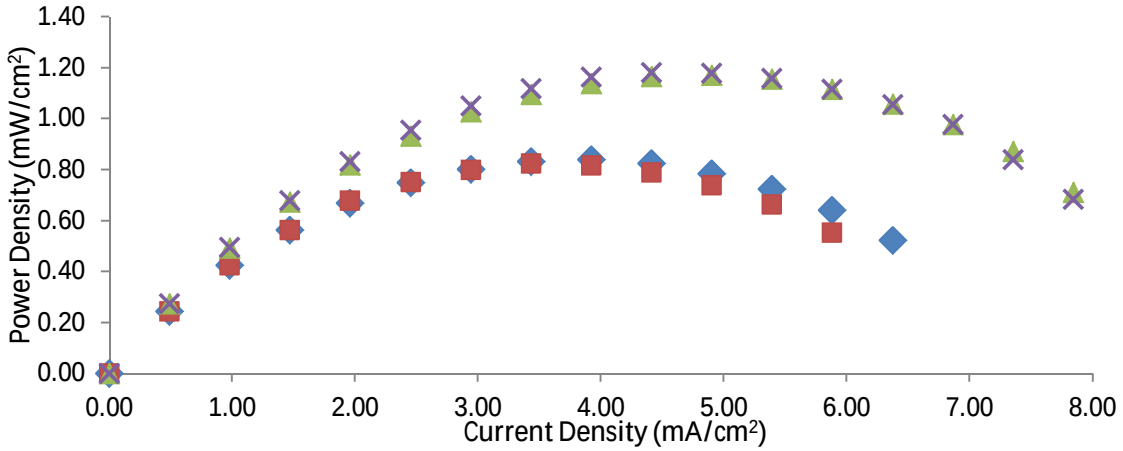

Figure 5.3.1: a) polarization curve and b) power density curve for the effect of cathode loading. Design parameters of the DEFC: anode catalyst - 2 mg/cm^2 of 40% Pt - 40% Sn/20% CB in 0.400 mm carbon cloth; cathode catalyst – carbon paper.

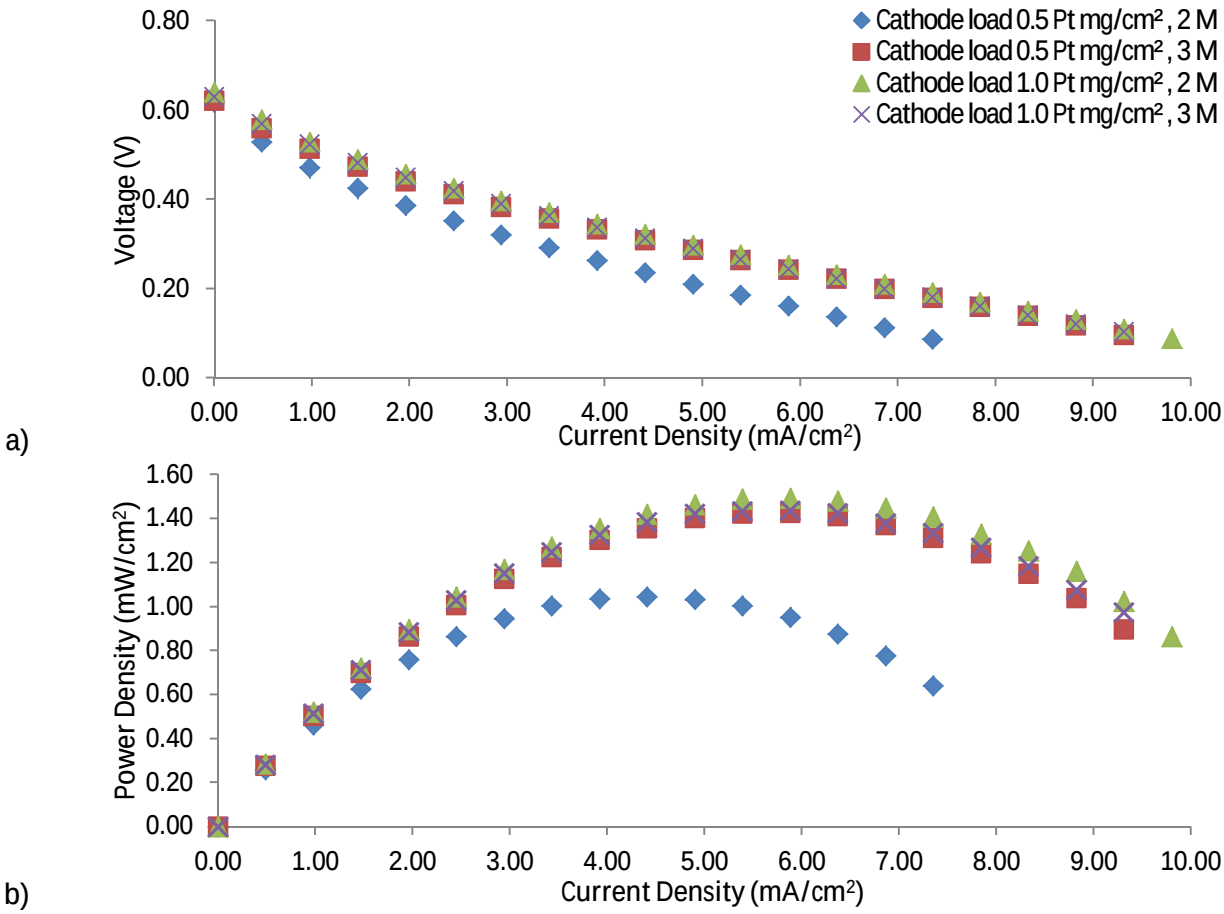

Figure 5.3.2: a) polarization curve and b) power density curve for the effect of cathode loading. Design parameters of the DEFC: anode catalyst – 2 mg/cm^2 of 40% Pt - 40% Sn/20% CB in 0.190 mm carbon paper; cathode catalyst – carbon paper.

5.4. Effect of anode binary catalyst metals

The binary catalysts tested were composed of Pt-Ru and Pt-Sn.

The Pt-Ru anode catalyst tested was a commercial product and the Pt-Sn catalyst was prepared by the LCM at FEUP and were both placed on CP GDLs.

The results obtained show that the best metal combination was the Pt-Sn as it was expected, Figure 5.4 . The ethanol concentration with the best results was the 2 M which is consistent with the conclusions of the subchapter 5.1. where it is stated that the best concentration to be used with CP as anode GDL is 2 M.

Pt-Sn catalyst performed much better than the Pt-Ru catalyst since, Ru is considered to be a more appropriate metal to use on the catalysis of methanol oxidation. The C-C bond, present on the ethanol molecule, modifies the oxidation reaction mechanism therefore, explaining the poor performance of the Pt-Ru catalyst.

Sn proved to be a metal with much more potential to accomplish the oxidation of ethanol because it provides adsorbed OH species that are crucial to promote the early stages of the oxidation mechanism.

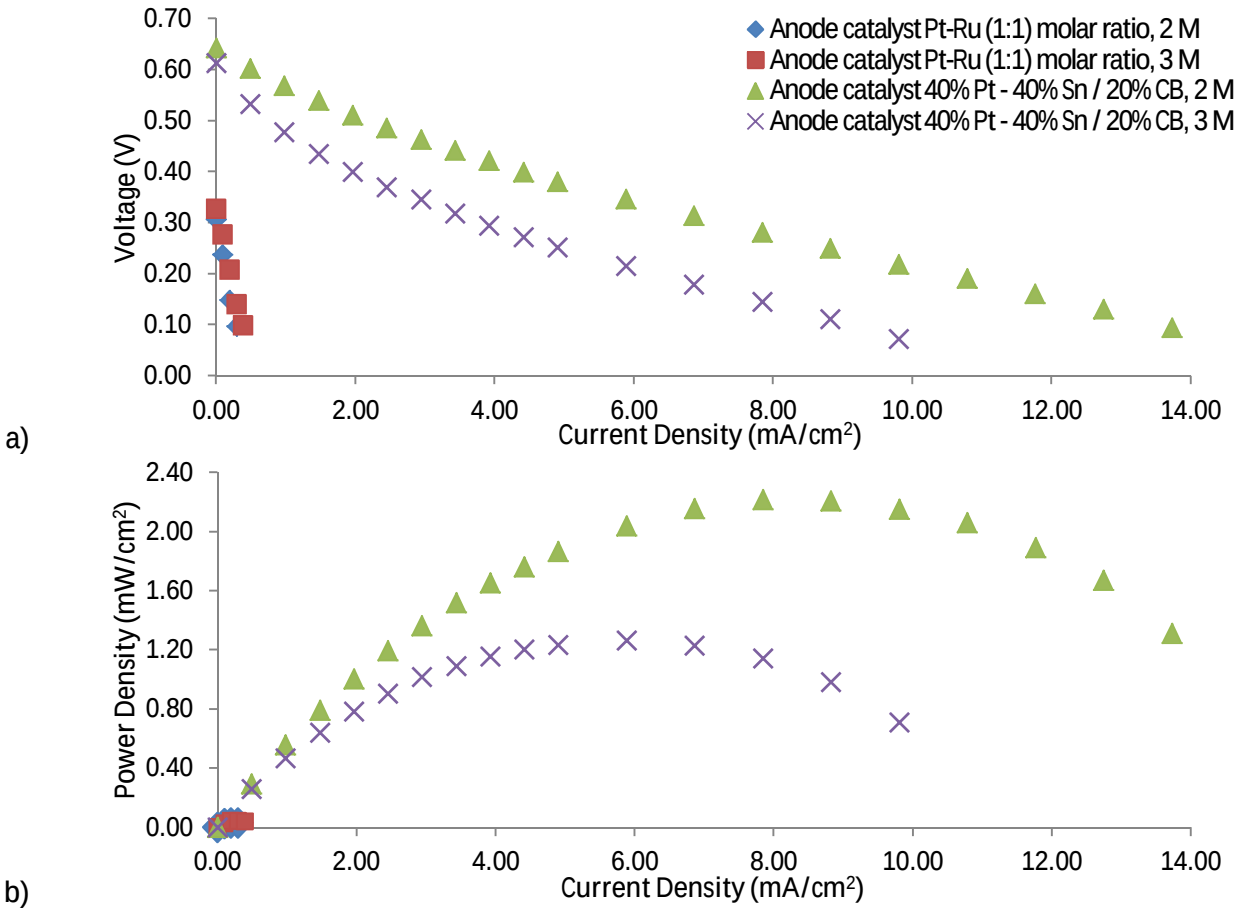

Figure 5.4: a) polarization curve and b) power density curve for the effect of cathode loading. Design parameters of the DEFC: anode catalyst – 3 mg/cm^2 carbon paper; cathode catalyst – 1.0 mg/cm^2 of Pt in 0.400 mm carbon paper.

5.5. Effect of anode catalyst loading

The influence of the anode catalyst loading was studied using two different loadings, 2 and 3 mg/cm^2, using the same anode catalyst, 40% Pt-40% Sn/20% CB.

It was expected that higher catalyst loadings would be better since there is a greater number of active sites available to perform the oxidation of ethanol. But, it is also a fact that higher catalyst loadings lead to higher thicknesses and higher ethanol resistance.

Analysing the results presented in Figures 5.5.1 and 5.5.2, using CC and CP as anode GDLs it can be seen that higher performances were achieved with higher ethanol oxidation rate which not only lowers the activation losses but, also the ethanol crossover.

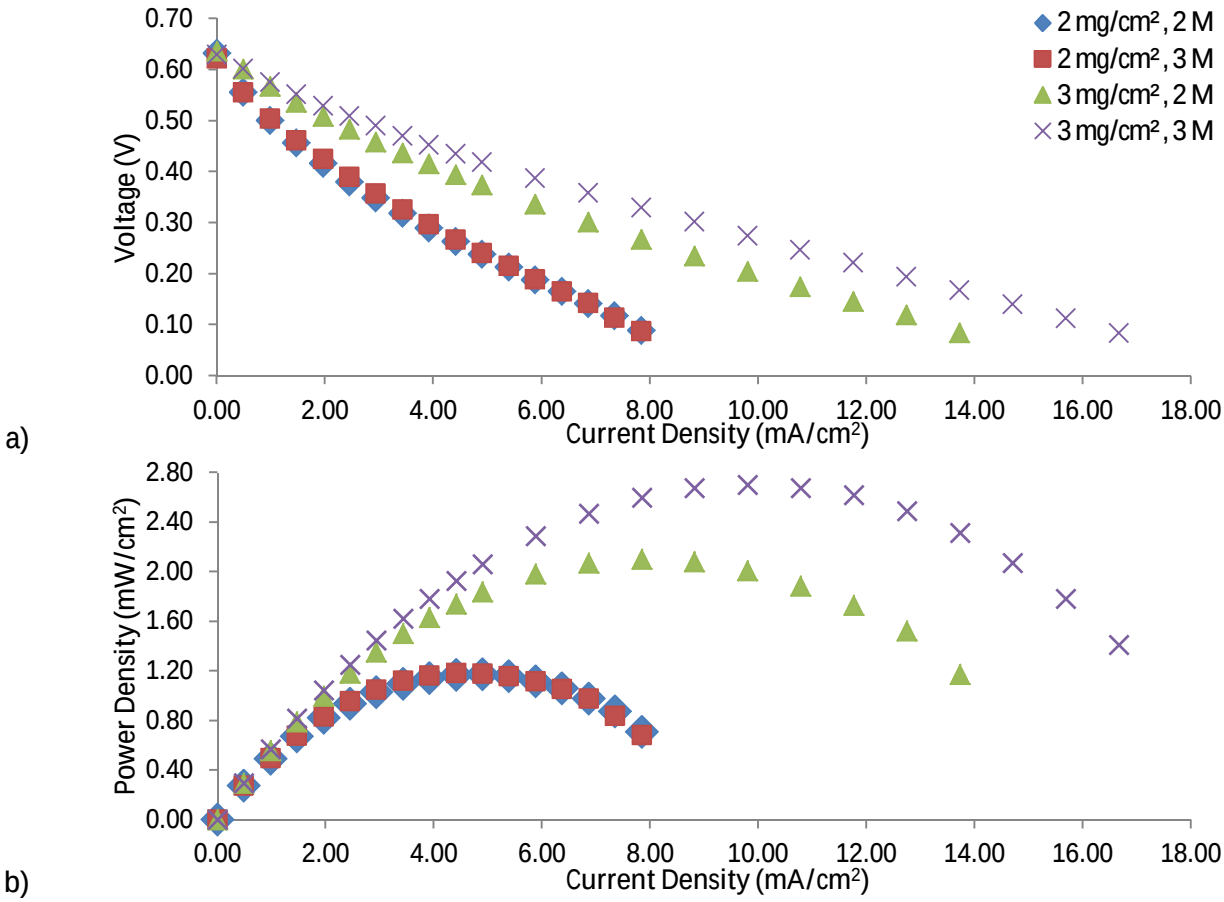

Figure 5.5.1: a) polarization curve and b) power density curve for the effect of anode catalyst loading. Design parameters of the DEFC: anode catalyst – 40% Pt - 40% Sn/20% CB in 0.400 mm carbon cloth; cathode catalyst – 1.0 mg/cm^2 of Pt in 0.400 mm carbon paper.

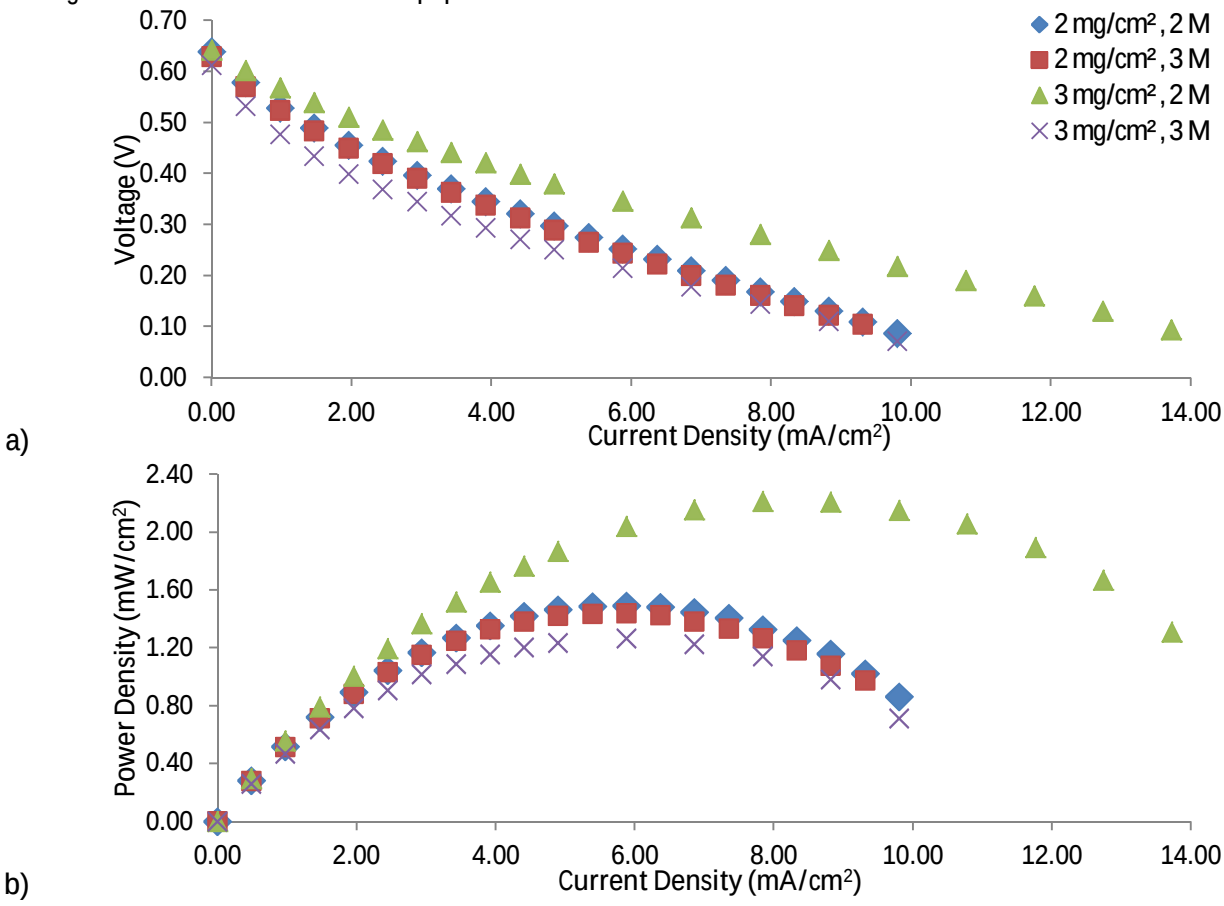

Figure 5.5.2: a) polarization curve and b) power density curve for the effect of anode catalyst loading. Design parameters of the DEFC: anode catalyst – 40% Pt - 40% Sn/20% CB in 0.190 mm carbon paper; cathode catalyst – 1.0 mg/cm^2 of Pt in 0.400 mm carbon paper.

5.6. Effect of anode catalyst metal percentage

In order to evaluate the effect of reducing the overall metal percentage of the anode catalyst two catalysts with the same metals, Pt and Sn, one having an overall metal percentage of 80%, 40% Pt-40% Sn/20% CB, and the other one having 40%, 20% Pt-20% Sn/60% CB, Figure 5.6.1 and Figure 5.6.2, were tested . The reduction of the metal percentage to half increases the percentage of carbon black (CB) that is added to the catalyst. Higher contents of CB can potentially improve the catalyst electronic conductivity and also lower its cost.

Unfortunately, the increase of CB percentage wasn't enough to compensate the lower metal percentage of the 20% Pt-20% Sn/60% CB catalyst and so, for both the combinations tested, using CC and CP as anode GDL, the best results were reached for the 40% Pt-40% Sn/20% CB catalyst.

These results proved that the presence of higher amounts of metal on the anode catalyst is beneficial to the oxidation reaction.

a)

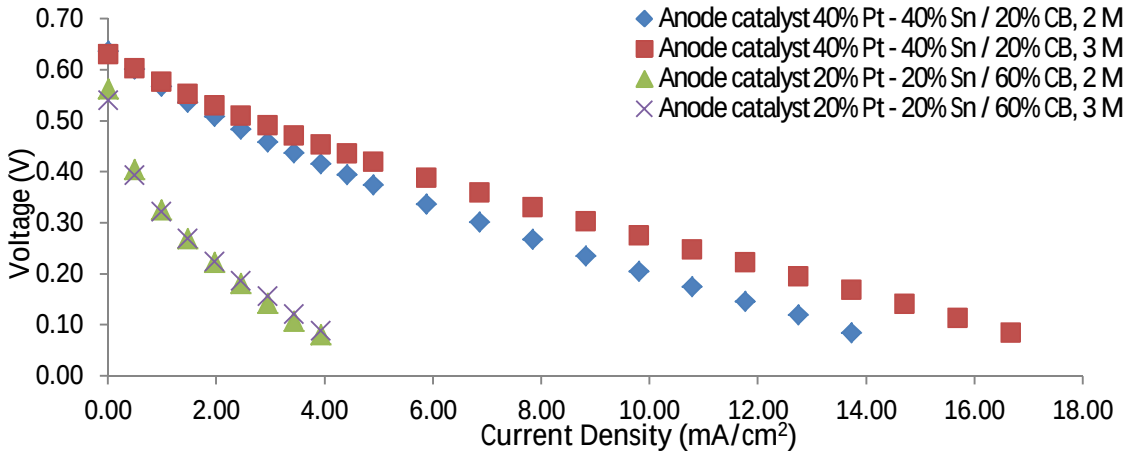

b)

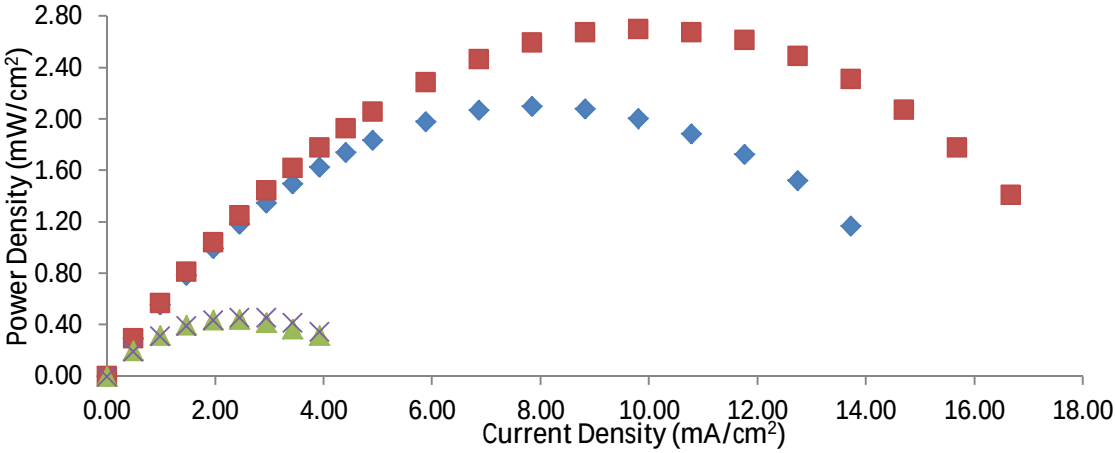

Figure 5.6.1: a) polarization curve and b) power density curve for the effect of anode catalyst metal percentages. Design parameters of the DEFC: anode catalyst – 3 mg/cm^2 in 0.400 mm carbon cloth; cathode catalyst – 1.0 mg/cm^2 of Pt in 0.400 mm carbon paper.

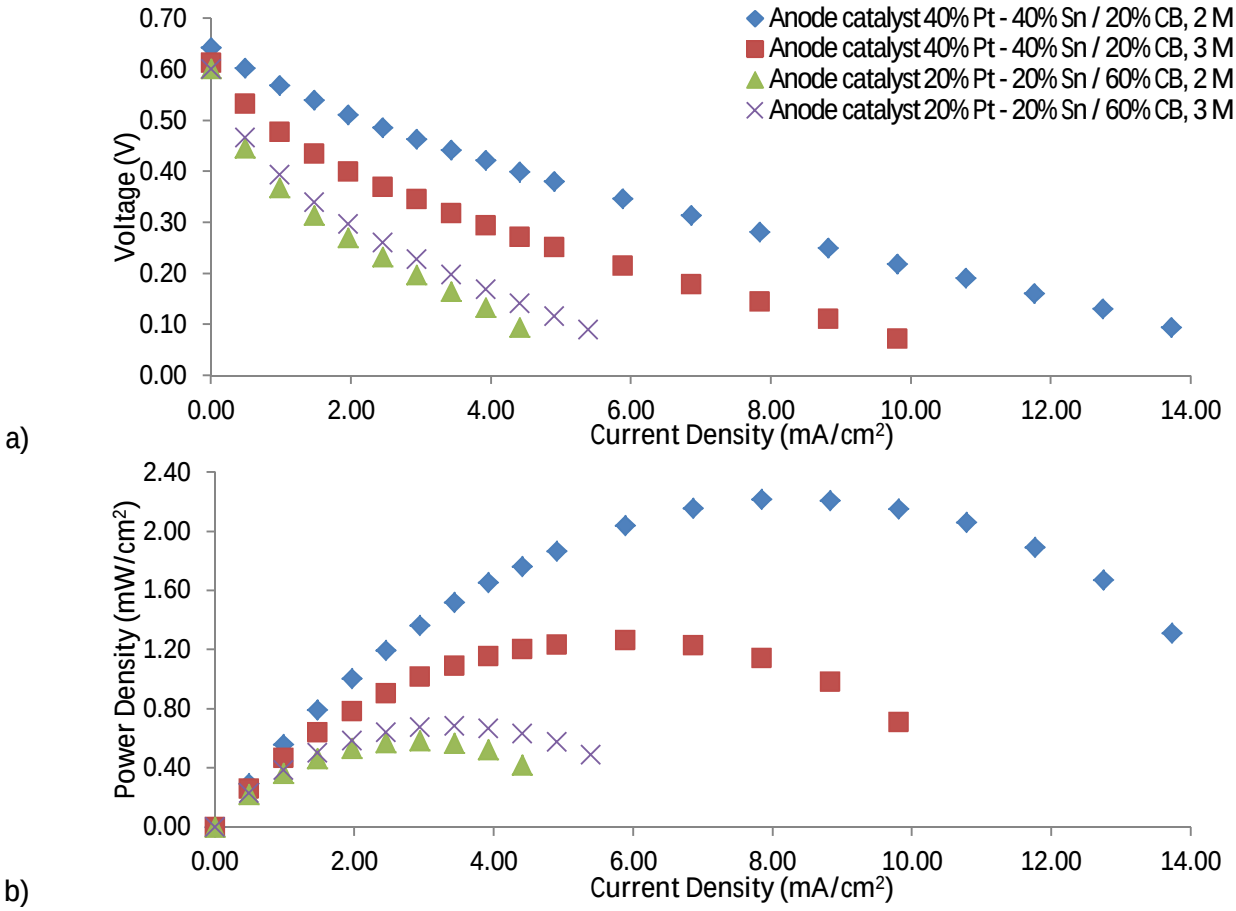

Figure 5.6.2: a) polarization curve and b) power density curve for the effect of anode catalyst metal percentages. Design parameters of the DEFC: anode catalyst – 3 mg/cm^2 in 0.190 mm carbon paper; cathode catalyst – 1.0 mg/cm^2 of Pt in 0.400 mm carbon paper.

5.7. Effect of anode gas diffusion layer material

To optimize the passive DEFC performance it's crucial to reduce the crossover of ethanol therefore, the fuel cell component that has the biggest impact on managing this natural phenomenon is the anode GDL.

The crossover phenomenon can be controlled by increasing the fuel mass transfer resistance by using different the anode GDL materials and using thicker GDLs. However, if the layer is too thick the amount of ethanol molecules that reach the anode catalyst will decrease, decreasing the ethanol oxidation rate and lowering the performance of the fuel cell thus, there must be established a compromise between the anode GDL thickness and the power output.

To study the effect of the anode diffusion layer material on the fuel cell performance, two types of materials were used: carbon cloth (CC) and carbon paper (CP), Figure 5.7, with two different thicknesses.

The results for the CC as GDL with a lower thickness and 3 M were the ones with the best performance. For that reason, from this point forward, the anode GDL used on the other tests was the 0.400 mm CC.

The lower thickness layer of CC obtained an overall best performance than the thicker layer because the increase of the mass transport resistance lowers not only, the amount of ethanol molecules that reach the catalyst layer but also, the removal rate of the reactional products.

In general the tests using CP as GDL achieved worse results than the ones using CC this could have happened due to the different fibber disposition of these materials, namely the porosity and tortuosity. The CP has a less porous and more tortuous structure than CC therefore, it is more difficult to ethanol molecules to reach the catalyst layer and also the production of CO_2 creates bubbles that get trapped on the CP structure blocking the access to the active sites.

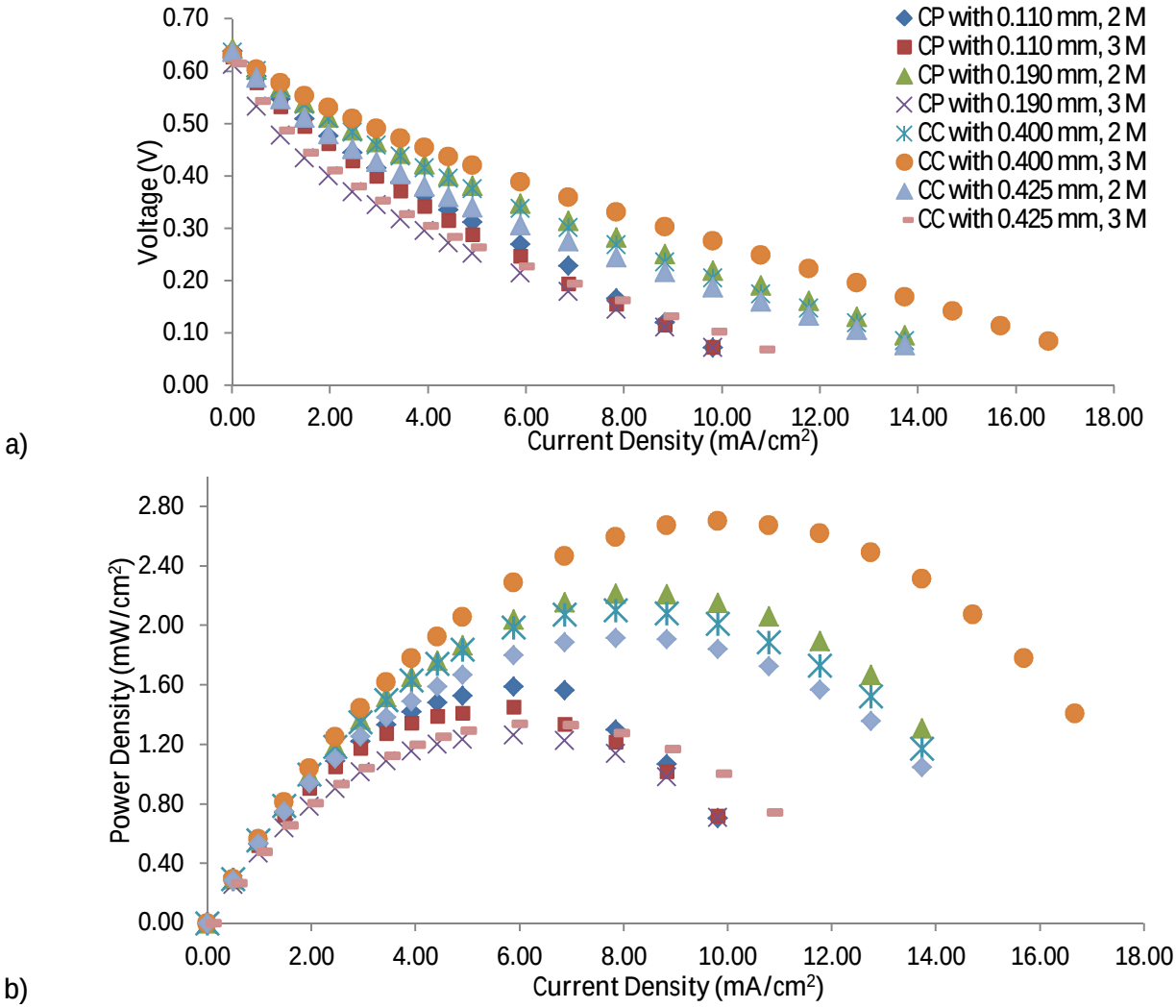

Figure 5.7: a) polarization curve and b) power density curve for the effect of anode gas diffusion layer material . Design parameters of the DEFC: anode catalyst – 3 mg/cm^2 of 40% Pt - 40% Sn/20% CB; cathode catalyst – 1.0 mg/cm^2 of Pt in 0.400 mm carbon paper.

5.8. Effect of anode catalyst metal percentage keeping an overall percentage of 40%

Even being aware of the fact that the 20% Pt-20% Sn/60% CB catalyst performed worse than the 40% Pt-40% Sn/20% CB (subchapter 5.6), it was decided to continue to study other catalyst proportions

maintaining the overall metal percentage of 40% to assess if slight changes on the percentages of each metal, Pt an Sn, would have an impact on the performance of the fuel cell and the results are presented in Figure 5.8.

The increase of Pt content on the anode catalyst, 60% Pt-40% Sn (24% Pt-16% Sn/60% CB) was beneficial to the oxidation reaction producing better results when compared to the 20% Pt-20% Sn/60% CB which is equivalent to 50% Pt-50% Sn for an overall metal percentage of 40%.

This proved to be a good decision because it was possible to improve the performance of the cell while maintaining relatively low amounts of metals which is good in terms of the catalyst costs.

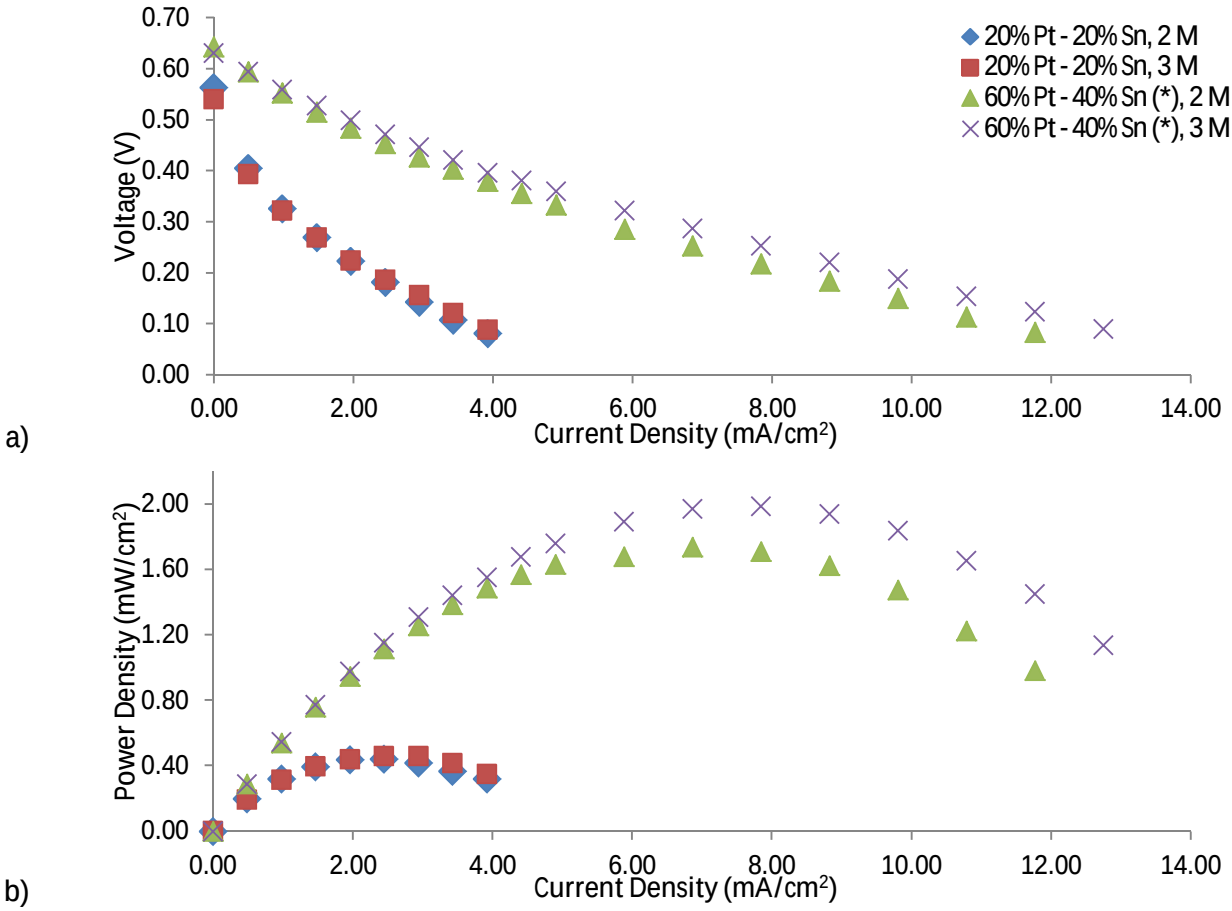

(*) - these metal percentages correspond to an overall metal percentage of 40%.

Figure 5.8: a) polarization curve and b) power density curve for the effect of binary anode catalyst metal percentage keeping an overall metal percentage of 40%. Design parameters of the DEFC: anode catalyst – 3 mg/cm^2 in 0.400 mm carbon cloth; cathode catalyst – 1.0 mg/cm^2 of Pt in 0.400 mm carbon paper.

5.9. Effect of ternary anode catalyst

Supported by the literature, Ni and Co were chosen to be the third metallic element to be added to the Pt-Sn-based binary anode catalyst to form the ternary catalysts. The presence of either one of these metals helps to strengthen the bond between the Pt and the carbon black (CB) improving the stability of the catalyst. For this reason these ternary catalysts should have higher performances than the ones obtained with the Pt-Sn binary anode catalyst.

Once more, the overall metal percentage, 40%, and Pt percentage, 60%, were kept constant. In order to introduce the third metal the Sn content was lowered 10% and the remaining percentage was for the new metal.

The result obtained, Figure 5.9, show that the binary anode catalyst 60% Pt-40% Sn (24% Pt-16% Sn/60% CB) had the best performance of the three however, the 60% Pt-30% Sn-10% Ni ternary catalyst (24% Pt-12% Sn-10% Ni /60% CB) was able to achieve similar the results.

a)

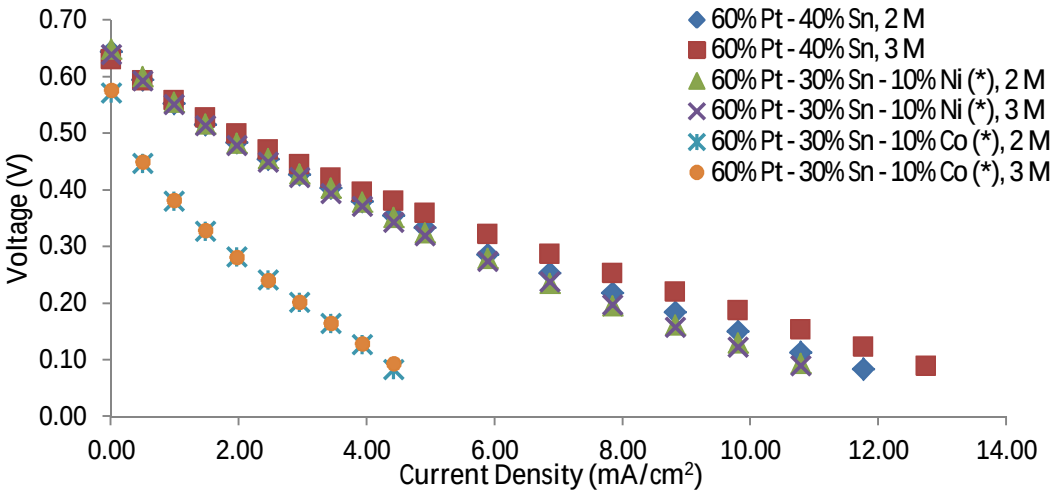

b)

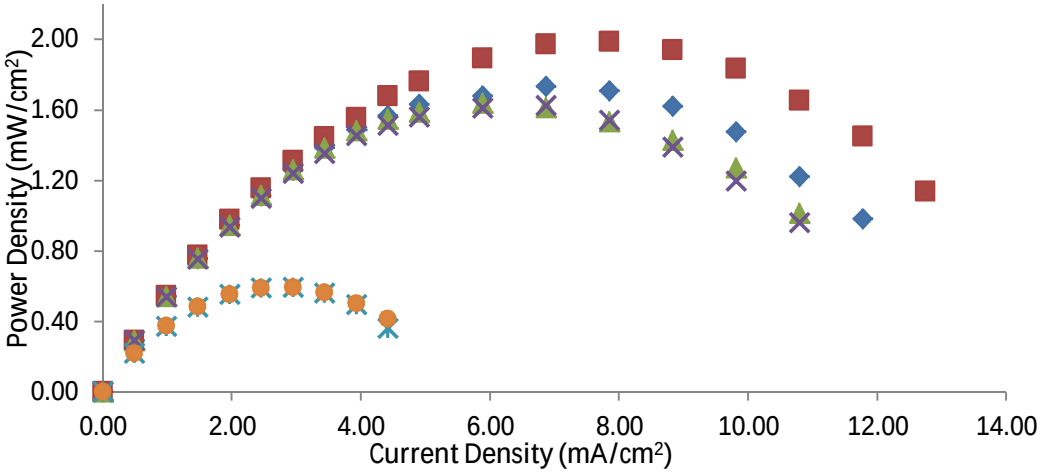

(*) - these metal percentages correspond to an overall metal percentage of 40%.

Figure 5.9: a) polarization curve and b) power density curve for the effect of ternary anode catalyst metals. Design parameters of the DEFC: anode catalyst – 3 mg/cm^2 in 0.400 mm carbon cloth; cathode catalyst – 1.0 mg/cm^2 of Pt in 0.400 mm carbon paper.

6. Conclusions and Suggestions to Future Work

6.1. Conclusions

The rapid grow of the energy needs leads to the necessity of find other power production processes since, it is from general knowledge that fossil fuels are a finite resource and their combustion releases greenhouse gases which contribute to the global warming. Therefore, it's crucial to study new ways of producing energy in an environmentally friendly and, preferably, in a renewable way and DEFCs are a technology that fits perfectly into these requirements.

The direct ethanol fuel cells are a promise power solution especially for portable applications with high efficiency and low environmental impact. The main objective of this work is to study the effect of operational conditions and design parameters on the fuel cell performance.

Through the polarization and power density curves it was possible to assess the fuel cell performance for configuration tested. So, based on the results reported on this work, it was possible to found the best combinations.

Analysing the effect of ethanol concentration the best results were achieved using a 3 M ethanol solution using CC as anode GDL and 2 M for the CP anode GDL, with maximum densities of 1.18 and 1.49 mW/cm^2, respectively.

Regarding the cathode side, the best performance was reached for the higher thickness and for a higher loading, achieving 1.18 mW/cm^2 using CC as anode GDL and 1.43 mW/cm^2 using CP as anode GDL.

The best metal combination for the binary anode catalyst was the Pt-Sn, and the better catalyst loading was 3 mg/cm^2. Also for the anode catalyst higher contents of metal, 40% Pt-40% Sn/20% CB, demonstrated to be beneficial using both CC and CP as anode GDLs, leading to maximum power densities of 2.70 and 2.22 mW/cm^2, respectively.

The influence of the anode GDL was studied by testing two types of materials with two different thicknesses and the best overall performance was achieved with the thinner CC, reaching 2.70 mW/cm^2.

Keeping the overall metal percentage on 40%, the anode catalyst with the highest Pt content, 60% Pt-40% Sn (24% Pt-16% Sn/60% CB), provided the best results achieving a maximum power density of 1.99 mW/cm^2.

The last effect studied was the addition of a third metallic element to the Pt-Sn binary anode catalyst. Comparing the performance of the Pt-Sn-Ni and the Pt-Sn-Co to the Pt-Sn, all with the same overall metal percentage, the binary catalyst was the best. Even though, the Pt-Sn-Ni performance was very close to the Pt-Sn catalyst, 1.64 mW/cm^2, and the results obtained with the Pt-Sn-Co catalyst were far from the expectations.

A general analysis of all the results reported allowed to conclude that the fuel cell configuration with the best performance, 2.70 mW/cm^2, was achieved using on the anode side a loading of 3 mg/cm^2 loading of 40% Pt-40% Sn/20% CB catalyst sprayed onto CC GDL with 0.400 mm and on the cathode side a Pt loading of 1 mg/cm^2 using CP as GDL with a thickness of 0.400 mm and a 3 M ethanol solution.

New design solutions will be proposed from the knowledge acquired from the experimental results contributing to the development of more efficient DEFCs.

6.2. Suggestions for Future Work

For future investigation, it is suggested the study of new proton exchange membrane materials, keep studying the anode binary catalyst, Pt-Sn, metal percentage and exploring other metal combinations to the ternary anode catalyst.

Finding new protons exchange materials could play an important role in decreasing the ethanol crossover and also lower the fuel cell costs.

This experimental study concluded that higher contents of Pt on the anode catalyst were beneficial but, perhaps it is important to study the metal content and the CB content in order to find a combination that allows the use of less Pt on the catalyst while keeping the same results.

New tests shall be done using the Pt-Sn-Co anode catalyst to assess if the results obtained were accurate or if there was some issue with the catalyst preparation that caused its unexpected performance.

It would be interesting to test other ternary catalysts, with different metal combinations, to see if it's possible to compensate the reduction in the Pt content incorporating and increasing the content of cheaper metals.

7. References

[1] M. Z. F. Kamarudin, S. K. Kamarudin, M. S. Masdar, and W. R. W. Daud, "Review: Direct ethanol fuel cells," *International Journal of Hydrogen Energy,* vol. 38, pp. 9438-9453, 2013.

[2] G. Hoogers, *Fuel Cell Technology Handbook*. Boca Raton [etc.]: CRC Press, 2003.

[3] F. A. C. M. d. Santos and F. M. S. M. d. Santos, "Células de combustível," 2004.

[4] S. Mekhilef, R. Saidur, and A. Safari, "Comparative study of different fuel cell technologies," *Renewable and Sustainable Energy Reviews,* vol. 16, pp. 981-989, 1// 2012.

[5] U. Lucia, "Overview on fuel cells," *Renewable and Sustainable Energy Reviews,* vol. 30, pp. 164-169, 2// 2014.

[6] R. C. O'Hayre, Suk-Won; Colella, Witney, Prinz, Fritz B., *Fuel Cell Fundamentals*. New York: John Wiley & Sons, 2006.

[7] U. S. D. o. E. N. E. T. L. Hawaii, *Fuel Cell Handbook* vol. Reprinted from the 2000 edition. Honolulu: University Press of the Pacific, 2005.

[8] O. Z. Sharaf and M. F. Orhan, "An overview of fuel cell technology: Fundamentals and applications," *Renewable and Sustainable Energy Reviews,* vol. 32, pp. 810-853, 4// 2014.

[9] J. Andújar and F. Segura, "Fuel cells: History and updating. A walk along two centuries," *Renewable and Sustainable Energy Reviews,* vol. 13, pp. 2309-2322, 2009.

[10] N. S. Suresh and S. Jayanti, "Cross-over and performance modeling of liquid-feed Polymer Electrolyte Membrane Direct Ethanol Fuel Cells," *International Journal of Hydrogen Energy,* vol. 36, pp. 14648-14658, 11// 2011.

[11] E. M. Cunha, J. Ribeiro, K. B. Kokoh, and A. R. de Andrade, "Preparation, characterization and application of Pt–Ru–Sn/C trimetallic electrocatalysts for ethanol oxidation in direct fuel cell," *International Journal of Hydrogen Energy,* vol. 36, pp. 11034-11042, 8// 2011.

[12] J. P. Pereira, D. S. Falcão, V. B. Oliveira, and A. M. F. R. Pinto, "Performance of a passive direct ethanol fuel cell," *Journal of Power Sources,* vol. 256, pp. 14-19, 2014.

[13] S. Song and P. Tsiakaras, "Recent progress in direct ethanol proton exchange membrane fuel cells (DE-PEMFCs)," *Applied Catalysis B: Environmental,* vol. 63, pp. 187-193, 2006.

[14] F. Vigier, C. Coutanceau, F. Hahn, E. M. Belgsir, and C. Lamy, "On the mechanism of ethanol electro-oxidation on Pt and PtSn catalysts: electrochemical and in situ IR reflectance spectroscopy studies," *Journal of Electroanalytical Chemistry,* vol. 563, pp. 81-89, 2004.

[15] G. M. Andreadis, A. K. M. Podias, and P. E. Tsiakaras, "The effect of the parasitic current on the Direct Ethanol PEM Fuel Cell Operation," *Journal of Power Sources,* vol. 181, pp. 214-227, 2008.

[16] E. Antolini, "Catalysts for direct ethanol fuel cells," *Journal of Power Sources,* vol. 170, pp. 1-12, 2007.

[17] J. Tayal, B. Rawat, and S. Basu, "Effect of addition of rhenium to Pt-based anode catalysts in electro-oxidation of ethanol in direct ethanol PEM fuel cell," *International Journal of Hydrogen Energy,* vol. 37, pp. 4597-4605, 3// 2012.

[18] J. Tayal, B. Rawat, and S. Basu, "Bi-metallic and tri-metallic Pt–Sn/C, Pt–Ir/C, Pt–Ir–Sn/C catalysts for electro-oxidation of ethanol in direct ethanol fuel cell," *International Journal of Hydrogen Energy,* vol. 36, pp. 14884-14897, 11// 2011.

[19] V. Alzate, K. Fatih, and H. Wang, "Effect of operating parameters and anode diffusion layer on the direct ethanol fuel cell performance," *Journal of Power Sources,* vol. 196, pp. 10625-10631, 2011.

[20] S. Beyhan, C. Coutanceau, J.-M. Léger, T. W. Napporn, and F. Kadırgan, "Promising anode candidates for direct ethanol fuel cell: Carbon supported PtSn-based trimetallic catalysts prepared by Bönnemann method," *International Journal of Hydrogen Energy,* vol. 38, pp. 6830-6841, 2013.

[21] K. Fatih, V. Neburchilov, V. Alzate, R. Neagu, and H. Wang, "Synthesis and characterization of quaternary PtRuIrSn/C electrocatalysts for direct ethanol fuel cells," *Journal of Power Sources,* vol. 195, pp. 7168-7175, 2010.

[22] S. P. S. Badwal, S. Giddey, A. Kulkarni, J. Goel, and S. Basu, "Direct ethanol fuel cells for transport and stationary applications – A comprehensive review," *Applied Energy,* vol. 145, pp. 80-103, 2015.

[23] M. Yekini Suberu, M. Wazir Mustafa, and N. Bashir, "Energy storage systems for renewable energy power sector integration and mitigation of intermittency," *Renewable and Sustainable Energy Reviews,* vol. 35, pp. 499-514, 7// 2014.

Appendix A

Table A.1 : Main characteristics of the different types of fuel cells [4, 5, 8, 23] .

Type of Fuel Cell	Electrolyte	Catalyst Type		Reaction	Charge Carrier	Fuel	Operation Temperature (°C)	Electrical Efficiency (%)	Maximum Power (kW)
		Anode	Cathode						
PEMFC	Nafion®	Platinum supported on carbon	Platinum supported on carbon	Oxidation: $H_2\,(g) \rightarrow 2H^+ + 2e^-$ Reduction: $^1/_2\ O_2\,(g) + 2H^+ + 2e^- \rightarrow H_2O\,(l)$	H^+	Hydrogen	60 – 100	40 – 60	250
AFC	Potassium hydroxide (KOH)	Nickel	Silver supported on carbon	Oxidation: $2H_2 + 4OH^- \rightarrow 4H_2O + 4e^-$ Reduction: $O_2 + 2H_2O + 4e^- \rightarrow 4OH^-$	OH^-	Hydrogen	0 – 230	60 – 70	20
PAFC	Concentrated liquid phosphoric acid (H_3PO_4) in silicon carbonate (SiC)	Platinum supported on carbon	Platinum supported on carbon	Oxidation: $2H_2 \rightarrow 4H^+ + 4e^-$ Reduction: $O_2 + 4H^+ + 4e^- \rightarrow 2H_2O$	H^+	Hydrogen	160 – 220	36 – 45	200
SOFC	Solid yttria-stabilized zirconia (YSZ)	Nickel-YSZ composite	Strontium-doped lanthanum manganite	Oxidation: $O^{2-} + H_2 \rightarrow H_2O + 2e^-$ Reduction: $^1/_2\ O_2 + 2e^- \rightarrow O^{2-}$	O^{2-}	•Methane •Hydrogen •Carbon monoxide	800 – 1000	55 – 65	3000
MCFC	Liquid alkali carbonate (Li_2CO_3, Na_2CO_3) in lithium aluminate ($LiAlO_2$)	Nickel-Chromium (NiCr)	Lithiated nickel oxide (NiO)	Oxidation: $H_2 + CO_3^{2-} \rightarrow H_2O + CO_2 + 2e^-$ Reduction: $^1/_2\ O_2 + CO_2 + 2e^- \rightarrow CO_3^{2-}$	CO_3^{2-}	• Hydrogen •Carbon monoxide •Natural gas •Propane	600 – 700	55 – 65	1000
DMFC	Nafion®	Platinum-Ruthenium supported on carbon	Platinum supported on carbon	Oxidation: $CH_3OH + H_2O \rightarrow CO_2 + 6H^+ + 6e^-$ Reduction: $^3/_2\ O_2 + 6H^+ + 6e^- \rightarrow 3H_2O$	H^+	Methanol	Ambient – – 110	35 – 60	100
DEFC	Nafion®	Platinum-Ruthenium supported on carbon	Platinum	Oxidation: $CH_3CH_2OH + 3H_2O \rightarrow 2CO_2 + 12H^+ + 12e^-$ Reduction: $3O_2 + 12H^+ + 12e^- \rightarrow 6H_2O$	H^+	Ethanol	Ambient – – 120	20 – 40	100

Appendix B

Effect of ethanol concentration

Table B.1: Cell design: membrane – Nafion 117; connector plates – stainless steel; anode catalyst – 2 mg/cm^2 of 40% Pt - 40% Sn/20% CB in 0.400 mm carbon cloth; cathode catalyst – 1.0 mg/cm^2 of Pt in 0.400 mm carbon paper.

1 M				2 M			
Current (A)	Current Density (mA/cm^2)	Voltage (V)	Power Density (mW/cm^2)	Current (A)	Current Density (mA/cm^2)	Voltage (V)	Power Density (mW/cm^2)
0.000	0.000	0.647	0.000	0.000	0.000	0.634	0.000
0.005	0.490	0.539	0.264	0.005	0.490	0.557	0.273
0.010	0.980	0.471	0.461	0.010	0.980	0.502	0.492
0.015	1.471	0.417	0.613	0.015	1.471	0.458	0.673
0.020	1.961	0.373	0.731	0.020	1.961	0.418	0.820
0.025	2.451	0.335	0.820	0.025	2.451	0.381	0.933
0.030	2.941	0.299	0.879	0.030	2.941	0.350	1.028
0.035	3.431	0.266	0.913	0.035	3.431	0.320	1.096
0.040	3.922	0.235	0.922	0.040	3.922	0.291	1.139
0.045	4.412	0.204	0.898	0.045	4.412	0.264	1.165
0.050	4.902	0.174	0.850	0.050	4.902	0.239	1.172
0.055	5.392	0.144	0.774	0.055	5.392	0.215	1.157
0.060	5.882	0.113	0.665	0.060	5.882	0.190	1.115
0.065	6.373	0.079	0.503	0.065	6.373	0.166	1.058
---	---	---	---	0.070	6.863	0.143	0.978
---	---	---	---	0.075	7.353	0.119	0.871
---	---	---	---	0.080	7.843	0.091	0.710

Table B.2: Cel design: membrane – Nafion 117; connector plates – stainless steel; anode catalyst – 2 mg/cm^2 of 40% Pt - 40% Sn/20% CB in 0.400 mm carbon cloth; cathode catalyst – 1.0 mg/cm^2 of Pt in 0.400 mm carbon paper.

3 M				4 M			
Current (A)	Current Density (mA/cm^2)	Voltage (V)	Power Density (mW/cm^2)	Current (A)	Current Density (mA/cm^2)	Voltage (V)	Power Density (mW/cm^2)
0.000	0.000	0.623	0.000	0.000	0.000	0.588	0.000
0.005	0.490	0.556	0.272	0.005	0.490	0.534	0.262
0.010	0.980	0.504	0.494	0.010	0.980	0.487	0.477
0.015	1.471	0.462	0.679	0.015	1.471	0.447	0.657
0.020	1.961	0.425	0.832	0.020	1.961	0.410	0.804
0.025	2.451	0.390	0.955	0.025	2.451	0.378	0.926
0.030	2.941	0.357	1.050	0.030	2.941	0.347	1.021
0.035	3.431	0.326	1.119	0.035	3.431	0.317	1.088
0.040	3.922	0.297	1.163	0.040	3.922	0.289	1.133
0.045	4.412	0.268	1.180	0.045	4.412	0.262	1.156
0.050	4.902	0.241	1.179	0.050	4.902	0.237	1.162
0.055	5.392	0.215	1.159	0.055	5.392	0.212	1.140
0.060	5.882	0.190	1.115	0.060	5.882	0.188	1.103
0.065	6.373	0.166	1.055	0.065	6.373	0.165	1.048
0.070	6.863	0.143	0.978	0.070	6.863	0.142	0.975
0.075	7.353	0.114	0.838	0.075	7.353	0.119	0.875

0.080	7.843	0.087	0.682	0.080	7.843	0.094	0.737

Table B.3: Cell design: membrane – Nafion 117; connector plates – stainless steel; anode catalyst – 2 mg/cm^2 of 40% Pt - 40% Sn/20% CB in 0.190 mm carbon paper; cathode catalyst – 1.0 mg/cm^2 of Pt in 0.400 mm carbon paper.

1M				2M			
Current (A)	Current Density (mA/cm^2)	Voltage (V)	Power Density (mW/cm^2)	Current (A)	Current Density (mA/cm^2)	Voltage (V)	Power Density (mW/cm^2)
0.000	0.000	0.656	0.000	0.000	0.000	0.640	0.000
0.005	0.490	0.570	0.279	0.005	0.490	0.580	0.284
0.010	0.980	0.512	0.501	0.010	0.980	0.530	0.519
0.015	1.471	0.467	0.686	0.015	1.471	0.490	0.721
0.020	1.961	0.428	0.838	0.020	1.961	0.457	0.895
0.025	2.451	0.391	0.958	0.025	2.451	0.426	1.043
0.030	2.941	0.359	1.054	0.030	2.941	0.397	1.168
0.035	3.431	0.328	1.125	0.035	3.431	0.371	1.271
0.040	3.922	0.298	1.167	0.040	3.922	0.346	1.355
0.045	4.412	0.269	1.187	0.045	4.412	0.322	1.421
0.050	4.902	0.242	1.184	0.050	4.902	0.299	1.463
0.055	5.392	0.214	1.151	0.055	5.392	0.276	1.488
0.060	5.882	0.185	1.085	0.060	5.882	0.254	1.491
0.065	6.373	0.160	1.020	0.065	6.373	0.233	1.482
0.070	6.863	0.128	0.878	0.070	6.863	0.211	1.448
0.075	7.353	0.105	0.768	0.075	7.353	0.192	1.408
---	---	---	---	0.080	7.843	0.170	1.329
---	---	---	---	0.085	8.333	0.151	1.254
---	---	---	---	0.090	8.824	0.132	1.160
---	---	---	---	0.095	9.314	0.110	1.025
---	---	---	---	0.100	9.804	0.088	0.863

Table B.4: Cell design: membrane – Nafion 117; connector plates – stainless steel; anode catalyst – 2 mg/cm^2 of 40% Pt - 40% Sn/20% CB in 0.190 mm carbon paper; cathode catalyst – 1.0 mg/cm^2 of Pt in 0.400 mm carbon paper.

3M			
Current (A)	Current Density (mA/cm^2)	Voltage (V)	Power Density (mW/cm^2)
0.000	0.000	0.630	0.000
0.005	0.490	0.571	0.280
0.010	0.980	0.524	0.514
0.015	1.471	0.484	0.711
0.020	1.961	0.450	0.882
0.025	2.451	0.420	1.029
0.030	2.941	0.392	1.151
0.035	3.431	0.364	1.247
0.040	3.922	0.339	1.327
0.045	4.412	0.314	1.383
0.050	4.902	0.290	1.422

0.055	5.392	0.266	1.434
0.060	5.882	0.245	1.438
0.065	6.373	0.224	1.424
0.070	6.863	0.201	1.379
0.075	7.353	0.182	1.335
0.080	7.843	0.162	1.267
0.085	8.333	0.142	1.183
0.090	8.824	0.122	1.076
0.095	9.314	0.105	0.973

Appendix C

Effect of cathode thickness

Table C.1: Celll design: membrane – Nafion 117; connector plates – stainless steel; anode catalyst – 2 mg/cm^2 of 40% Pt - 40% Sn/20% CB in 0.400 mm carbon cloth; cathode catalyst – 0.5 mg/cm^2 of Pt in 0.400 mm carbon paper.

2M				3M			
Current (A)	Current Density (mA/cm^2)	Voltage (V)	Power Density (mW/cm^2)	Current (A)	Current Density (mA/cm^2)	Voltage (V)	Power Density (mW/cm^2)
0.000	0.000	0.606	0.000	0.000	0.000	0.602	0.000
0.005	0.490	0.497	0.243	0.005	0.490	0.498	0.244
0.010	0.980	0.432	0.424	0.010	0.980	0.434	0.425
0.015	1.471	0.382	0.562	0.015	1.471	0.383	0.563
0.020	1.961	0.341	0.668	0.020	1.961	0.346	0.677
0.025	2.451	0.305	0.748	0.025	2.451	0.307	0.751
0.030	2.941	0.273	0.801	0.030	2.941	0.272	0.800
0.035	3.431	0.243	0.832	0.035	3.431	0.240	0.824
0.040	3.922	0.214	0.839	0.040	3.922	0.209	0.818
0.045	4.412	0.187	0.823	0.045	4.412	0.179	0.788
0.050	4.902	0.160	0.784	0.050	4.902	0.151	0.738
0.055	5.392	0.134	0.723	0.055	5.392	0.123	0.663
0.060	5.882	0.109	0.641	0.060	5.882	0.094	0.553
0.065	6.373	0.082	0.523	---	---	---	---

Table C.2: Cell design: membrane – Nafion 117; connector plates – stainless steel; anode catalyst – 2 mg/cm^2 of 40% Pt - 40% Sn/20% CB in 0.400 mm carbon cloth; cathode catalyst – 0.5 mg/cm^2 of Pt in 0.270 mm carbon paper.

2M				3M			
Current (A)	Current Density (mA/cm^2)	Voltage (V)	Power Density (mW/cm^2)	Current (A)	Current Density (mA/cm^2)	Voltage (V)	Power Density (mW/cm^2)
0.000	0.000	0.610	0.000	0.000	0.000	0.592	0.000
0.005	0.490	0.493	0.242	0.005	0.490	0.478	0.234
0.010	0.980	0.425	0.416	0.010	0.980	0.413	0.404
0.015	1.471	0.371	0.546	0.015	1.471	0.361	0.530
0.020	1.961	0.325	0.636	0.020	1.961	0.315	0.618
0.025	2.451	0.281	0.689	0.025	2.451	0.273	0.669
0.030	2.941	0.241	0.707	0.030	2.941	0.233	0.685
0.035	3.431	0.213	0.731	0.035	3.431	0.199	0.681
0.040	3.922	0.178	0.696	0.040	3.922	0.165	0.645
0.045	4.412	0.147	0.649	0.045	4.412	0.135	0.593
0.050	4.902	0.112	0.549	0.050	4.902	0.097	0.475
0.055	5.392	0.080	0.431	---	---	---	---

Table C.3: Cell design: membrane – Nafion 117; connector plates – stainless steel; anode catalyst – 2 mg/cm^2 of 40% Pt - 40% Sn/20% CB in 0.190 mm carbon paper; cathode catalyst – 0.5 mg/cm^2 of Pt in 0.400 mm carbon paper.

2M				3M			
Current (A)	Current Density (mA/cm^2)	Voltage (V)	Power Density (mW/cm^2)	Current (A)	Current Density (mA/cm^2)	Voltage (V)	Power Density (mW/cm^2)
0.000	0.000	0.618	0.000	0.000	0.000	0.621	0.000
0.005	0.490	0.529	0.259	0.005	0.490	0.560	0.274
0.010	0.980	0.472	0.462	0.010	0.980	0.513	0.502
0.015	1.471	0.426	0.626	0.015	1.471	0.474	0.696
0.020	1.961	0.387	0.758	0.020	1.961	0.440	0.863
0.025	2.451	0.352	0.863	0.025	2.451	0.411	1.006
0.030	2.941	0.321	0.944	0.030	2.941	0.383	1.126
0.035	3.431	0.292	1.002	0.035	3.431	0.357	1.225
0.040	3.922	0.264	1.035	0.040	3.922	0.332	1.302
0.045	4.412	0.237	1.043	0.045	4.412	0.308	1.357
0.050	4.902	0.211	1.032	0.050	4.902	0.286	1.402
0.055	5.392	0.186	1.003	0.055	5.392	0.264	1.424
0.060	5.882	0.162	0.950	0.060	5.882	0.243	1.426
0.065	6.373	0.138	0.876	0.065	6.373	0.222	1.412
0.070	6.863	0.113	0.775	0.070	6.863	0.200	1.369
0.075	7.353	0.087	0.640	0.075	7.353	0.179	1.313
---	---	---	---	0.080	7.843	0.159	1.243
---	---	---	---	0.085	8.333	0.138	1.150
---	---	---	---	0.090	8.824	0.118	1.037
---	---	---	---	0.095	9.314	0.096	0.894

Table C.4: Cel design: membrane – Nafion 117; connector plates – stainless steel; anode catalyst – 2 mg/cm^2 of 40% Pt - 40% Sn/20% CB in 0.190 mm carbon paper; cathode catalyst – 0.5 mg/cm^2 of Pt in 0.270 mm carbon paper.

2M				3M			
Current (A)	Current Density (mA/cm^2)	Voltage (V)	Power Density (mW/cm^2)	Current (A)	Current Density (mA/cm^2)	Voltage (V)	Power Density (mW/cm^2)
0.000	0.000	0.586	0.000	0.000	0.000	0.577	0.000
0.005	0.490	0.459	0.225	0.005	0.490	0.454	0.222
0.010	0.980	0.389	0.381	0.010	0.980	0.388	0.380
0.015	1.471	0.335	0.492	0.015	1.471	0.337	0.496
0.020	1.961	0.289	0.567	0.020	1.961	0.293	0.575
0.025	2.451	0.247	0.605	0.025	2.451	0.254	0.621
0.030	2.941	0.209	0.615	0.030	2.941	0.217	0.637
0.035	3.431	0.173	0.594	0.035	3.431	0.183	0.626
0.040	3.922	0.139	0.543	0.040	3.922	0.149	0.584
0.045	4.412	0.106	0.465	0.045	4.412	0.118	0.521
0.050	4.902	0.073	0.355	0.050	4.902	0.085	0.417

Appendix D

Effect of cathode catalyst loading

Table D.1: Cel design: membrane – Nafion 117; connector plates – stainless steel; anode catalyst – 2 mg/cm^2 of 40% Pt - 40% Sn/20% CB in 0.400 mm carbon cloth; cathode catalyst – 0.5 mg/cm^2 of Pt in 0.400 mm carbon paper.

2M				3M			
Current (A)	Current Density (mA/cm^2)	Voltage (V)	Power Density (mW/cm^2)	Current (A)	Current Density (mA/cm^2)	Voltage (V)	Power Density (mW/cm^2)
0.000	0.000	0.606	0.000	0.000	0.000	0.602	0.000
0.005	0.490	0.497	0.243	0.005	0.490	0.498	0.244
0.010	0.980	0.432	0.424	0.010	0.980	0.434	0.425
0.015	1.471	0.382	0.562	0.015	1.471	0.383	0.563
0.020	1.961	0.341	0.668	0.020	1.961	0.346	0.677
0.025	2.451	0.305	0.748	0.025	2.451	0.307	0.751
0.030	2.941	0.273	0.801	0.030	2.941	0.272	0.800
0.035	3.431	0.243	0.832	0.035	3.431	0.240	0.824
0.040	3.922	0.214	0.839	0.040	3.922	0.209	0.818
0.045	4.412	0.187	0.823	0.045	4.412	0.179	0.788
0.050	4.902	0.160	0.784	0.050	4.902	0.151	0.738
0.055	5.392	0.134	0.723	0.055	5.392	0.123	0.663
0.060	5.882	0.109	0.641	0.060	5.882	0.094	0.553
0.065	6.373	0.082	0.523	---	---	---	---

Table D.2: Cel design: membrane – Nafion 117; connector plates – stainless steel; anode catalyst – 2 mg/cm^2 of 40% Pt - 40% Sn/20% CB in 0.400 mm carbon cloth; cathode catalyst – 1.0 mg/cm^2 of Pt in 0.400 mm carbon paper.

2M				3M			
Current (A)	Current Density (mA/cm^2)	Voltage (V)	Power Density (mW/cm^2)	Current (A)	Current Density (mA/cm^2)	Voltage (V)	Power Density (mW/cm^2)
0.000	0.000	0.634	0.000	0.000	0.000	0.623	0.000
0.005	0.490	0.557	0.273	0.005	0.490	0.556	0.272
0.010	0.980	0.502	0.492	0.010	0.980	0.504	0.494
0.015	1.471	0.458	0.673	0.015	1.471	0.462	0.679
0.020	1.961	0.418	0.820	0.020	1.961	0.425	0.832
0.025	2.451	0.381	0.933	0.025	2.451	0.390	0.955
0.030	2.941	0.350	1.028	0.030	2.941	0.357	1.050
0.035	3.431	0.320	1.096	0.035	3.431	0.326	1.119
0.040	3.922	0.291	1.139	0.040	3.922	0.297	1.163
0.045	4.412	0.264	1.165	0.045	4.412	0.268	1.180
0.050	4.902	0.239	1.172	0.050	4.902	0.241	1.179
0.055	5.392	0.215	1.157	0.055	5.392	0.215	1.159
0.060	5.882	0.190	1.115	0.060	5.882	0.190	1.115
0.065	6.373	0.166	1.058	0.065	6.373	0.166	1.055
0.070	6.863	0.143	0.978	0.070	6.863	0.143	0.978
0.075	7.353	0.119	0.871	0.075	7.353	0.114	0.838
0.080	7.843	0.091	0.710	0.080	7.843	0.087	0.682

Table D.3: Cell design: membrane – Nafion 117; connector plates – stainless steel; anode catalyst – 2 mg/cm^2 of 40% Pt - 40% Sn/20% CB in 0.190 mm carbon paper; cathode catalyst – 0.5 mg/cm^2 of Pt in 0.400 mm carbon paper.

2M				3M			
Current (A)	Current Density (mA/cm^2)	Voltage (V)	Power Density (mW/cm^2)	Current (A)	Current Density (mA/cm^2)	Voltage (V)	Power Density (mW/cm^2)
0.000	0.000	0.618	0.000	0.000	0.000	0.621	0.000
0.005	0.490	0.529	0.259	0.005	0.490	0.560	0.274
0.010	0.980	0.472	0.462	0.010	0.980	0.513	0.502
0.015	1.471	0.426	0.626	0.015	1.471	0.474	0.696
0.020	1.961	0.387	0.758	0.020	1.961	0.440	0.863
0.025	2.451	0.352	0.863	0.025	2.451	0.411	1.006
0.030	2.941	0.321	0.944	0.030	2.941	0.383	1.126
0.035	3.431	0.292	1.002	0.035	3.431	0.357	1.225
0.040	3.922	0.264	1.035	0.040	3.922	0.332	1.302
0.045	4.412	0.237	1.043	0.045	4.412	0.308	1.357
0.050	4.902	0.211	1.032	0.050	4.902	0.286	1.402
0.055	5.392	0.186	1.003	0.055	5.392	0.264	1.424
0.060	5.882	0.162	0.950	0.060	5.882	0.243	1.426
0.065	6.373	0.138	0.876	0.065	6.373	0.222	1.412
0.070	6.863	0.113	0.775	0.070	6.863	0.200	1.369
0.075	7.353	0.087	0.640	0.075	7.353	0.179	1.313
---	---	---	---	0.080	7.843	0.159	1.243
---	---	---	---	0.085	8.333	0.138	1.150
---	---	---	---	0.090	8.824	0.118	1.037
---	---	---	---	0.095	9.314	0.096	0.894

Table D.4: Cell design: membrane – Nafion 117; connector plates – stainless steel; anode catalyst – 2 mg/cm^2 of 40% Pt - 40% Sn/20% CB in 0.190 mm carbon paper; cathode catalyst – 1.0 mg/cm^2 of Pt in 0.400 mm carbon paper.

2M				3M			
Current (A)	Current Density (mA/cm^2)	Voltage (V)	Power Density (mW/cm^2)	Current (A)	Current Density (mA/cm^2)	Voltage (V)	Power Density (mW/cm^2)
0.000	0.000	0.640	0.000	0.000	0.000	0.630	0.000
0.005	0.490	0.580	0.284	0.005	0.490	0.571	0.280
0.010	0.980	0.530	0.519	0.010	0.980	0.524	0.514
0.015	1.471	0.490	0.721	0.015	1.471	0.484	0.711
0.020	1.961	0.457	0.895	0.020	1.961	0.450	0.882
0.025	2.451	0.426	1.043	0.025	2.451	0.420	1.029
0.030	2.941	0.397	1.168	0.030	2.941	0.392	1.151
0.035	3.431	0.371	1.271	0.035	3.431	0.364	1.247
0.040	3.922	0.346	1.355	0.040	3.922	0.339	1.327
0.045	4.412	0.322	1.421	0.045	4.412	0.314	1.383
0.050	4.902	0.299	1.463	0.050	4.902	0.290	1.422
0.055	5.392	0.276	1.488	0.055	5.392	0.266	1.434
0.060	5.882	0.254	1.491	0.060	5.882	0.245	1.438
0.065	6.373	0.233	1.482	0.065	6.373	0.224	1.424
0.070	6.863	0.211	1.448	0.070	6.863	0.201	1.379
0.075	7.353	0.192	1.408	0.075	7.353	0.182	1.335
0.080	7.843	0.170	1.329	0.080	7.843	0.162	1.267

0.085	8.333	0.151	1.254	0.085	8.333	0.142	1.183
0.090	8.824	0.132	1.160	0.090	8.824	0.122	1.076
0.095	9.314	0.110	1.025	0.095	9.314	0.105	0.973
0.100	9.804	0.088	0.863	---	---	---	---

Appendix E

Effect of binary anode catalyst metals

Table E.1: Cell design: membrane – Nafion 117; connector plates – stainless steel; anode catalyst – Pt-Ru (1:1) 3 mg/cm^2 carbon paper; cathode catalyst – 1.0 mg/cm^2 of Pt in 0.400 mm carbon paper.

2M				3M			
Current (A)	Current Density (mA/cm^2)	Voltage (V)	Power Density (mW/cm^2)	Current (A)	Current Density (mA/cm^2)	Voltage (V)	Power Density (mW/cm^2)
0.000	0.000	0.307	0.000	0.000	0.000	0.327	0.000
0.001	0.098	0.238	0.023	0.001	0.098	0.277	0.027
0.002	0.196	0.149	0.029	0.002	0.196	0.209	0.041
0.003	0.294	0.098	0.029	0.003	0.294	0.141	0.041
---	---	---	---	0.004	0.392	0.099	0.039

Table E.2: Cell design: membrane – Nafion 117; connector plates – stainless steel; anode catalyst – 3 mg/cm^2 of 40% Pt - 40% Sn/20% CB in 0.190 mm carbon paper; cathode catalyst – 1.0 mg/cm^2 of Pt in 0.400 mm carbon paper.

2M				3M			
Current (A)	Current Density (mA/cm^2)	Voltage (V)	Power Density (mW/cm^2)	Current (A)	Current Density (mA/cm^2)	Voltage (V)	Power Density (mW/cm^2)
0.000	0.000	0.643	0.000	0.000	0.000	0.613	0.000
0.005	0.490	0.604	0.296	0.005	0.490	0.533	0.261
0.010	0.980	0.570	0.558	0.010	0.980	0.478	0.468
0.015	1.471	0.540	0.794	0.015	1.471	0.435	0.639
0.020	1.961	0.512	1.004	0.020	1.961	0.400	0.784
0.025	2.451	0.487	1.194	0.025	2.451	0.370	0.906
0.030	2.941	0.465	1.366	0.030	2.941	0.346	1.016
0.035	3.431	0.443	1.518	0.035	3.431	0.318	1.091
0.040	3.922	0.422	1.655	0.040	3.922	0.295	1.157
0.045	4.412	0.400	1.765	0.045	4.412	0.273	1.202
0.050	4.902	0.381	1.868	0.050	4.902	0.252	1.235
0.060	5.882	0.347	2.041	0.060	5.882	0.215	1.265
0.070	6.863	0.315	2.158	0.070	6.863	0.179	1.228
0.080	7.843	0.283	2.216	0.080	7.843	0.146	1.141
0.090	8.824	0.251	2.210	0.090	8.824	0.112	0.984
0.100	9.804	0.220	2.152	0.100	9.804	0.073	0.711
0.110	10.784	0.191	2.060	---	---	---	---
0.120	11.765	0.161	1.894	---	---	---	---
0.130	12.745	0.131	1.670	---	---	---	---
0.140	13.725	0.096	1.311	---	---	---	---

Appendix F

Effect of binary anode catalyst loading

Table F.1: Cell design: membrane – Nafion 117; connector plates – stainless steel; anode catalyst – 2 mg/cm^2 of 40% Pt - 40% Sn/20% CB in 0.400 mm carbon cloth; cathode catalyst – 1.0 mg/cm^2 of Pt in 0.400 mm carbon paper.

2M				3M			
Current (A)	Current Density (mA/cm^2)	Voltage (V)	Power Density (mW/cm^2)	Current (A)	Current Density (mA/cm^2)	Voltage (V)	Power Density (mW/cm^2)
0.000	0.000	0.634	0.000	0.000	0.000	0.623	0.000
0.005	0.490	0.557	0.273	0.005	0.490	0.556	0.272
0.010	0.980	0.502	0.492	0.010	0.980	0.504	0.494
0.015	1.471	0.458	0.673	0.015	1.471	0.462	0.679
0.020	1.961	0.418	0.820	0.020	1.961	0.425	0.832
0.025	2.451	0.381	0.933	0.025	2.451	0.390	0.955
0.030	2.941	0.350	1.028	0.030	2.941	0.357	1.050
0.035	3.431	0.320	1.096	0.035	3.431	0.326	1.119
0.040	3.922	0.291	1.139	0.040	3.922	0.297	1.163
0.045	4.412	0.264	1.165	0.045	4.412	0.268	1.180
0.050	4.902	0.239	1.172	0.050	4.902	0.241	1.179
0.055	5.392	0.215	1.157	0.055	5.392	0.215	1.159
0.060	5.882	0.190	1.115	0.060	5.882	0.190	1.115
0.065	6.373	0.166	1.058	0.065	6.373	0.166	1.055
0.070	6.863	0.143	0.978	0.070	6.863	0.143	0.978
0.075	7.353	0.119	0.871	0.075	7.353	0.114	0.838
0.080	7.843	0.091	0.710	0.080	7.843	0.087	0.682

Table F.2: Cell design: membrane – Nafion 117; connector plates – stainless steel; anode catalyst – 3 mg/cm^2 of 40% Pt - 40% Sn/20% CB in 0.400 mm carbon cloth; cathode catalyst – 1.0 mg/cm^2 of Pt in 0.400 mm carbon paper.

2M				3M			
Current (A)	Current Density (mA/cm^2)	Voltage (V)	Power Density (mW/cm^2)	Current (A)	Current Density (mA/cm^2)	Voltage (V)	Power Density (mW/cm^2)
0.000	0.000	0.637	0.000	0.000	0.000	0.631	0.000
0.005	0.490	0.602	0.295	0.005	0.490	0.603	0.296
0.010	0.980	0.568	0.557	0.010	0.980	0.578	0.566
0.015	1.471	0.537	0.789	0.015	1.471	0.554	0.814
0.020	1.961	0.509	0.998	0.020	1.961	0.531	1.041
0.025	2.451	0.484	1.185	0.025	2.451	0.510	1.250
0.030	2.941	0.460	1.351	0.030	2.941	0.491	1.444
0.035	3.431	0.438	1.501	0.035	3.431	0.472	1.620
0.040	3.922	0.416	1.631	0.040	3.922	0.454	1.780
0.045	4.412	0.395	1.743	0.045	4.412	0.437	1.926
0.050	4.902	0.375	1.838	0.050	4.902	0.420	2.059
0.060	5.882	0.338	1.985	0.060	5.882	0.389	2.288
0.070	6.863	0.302	2.073	0.070	6.863	0.360	2.467
0.080	7.843	0.268	2.102	0.080	7.843	0.331	2.596
0.090	8.824	0.236	2.082	0.090	8.824	0.303	2.674
0.100	9.804	0.205	2.010	0.100	9.804	0.276	2.701

0.110	10.784	0.175	1.887	0.110	10.784	0.248	2.675
0.120	11.765	0.147	1.729	0.120	11.765	0.223	2.618
0.130	12.745	0.120	1.523	0.130	12.745	0.196	2.492
0.140	13.725	0.086	1.174	0.140	13.725	0.169	2.313
---	---	---	---	0.150	14.706	0.141	2.074
---	---	---	---	0.160	15.686	0.114	1.780
---	---	---	---	0.170	16.667	0.085	1.408

Table F.3: Cell design: membrane – Nafion 117; connector plates – stainless steel; anode catalyst – 2 mg/cm^2 of 40% Pt - 40% Sn/20% CB in 0.190 mm carbon paper; cathode catalyst – 1.0 mg/cm^2 of Pt in 0.400 mm carbon paper.

2M				3M			
Current (A)	Current Density (mA/cm^2)	Voltage (V)	Power Density (mW/cm^2)	Current (A)	Current Density (mA/cm^2)	Voltage (V)	Power Density (mW/cm^2)
0.000	0.000	0.640	0.000	0.000	0.000	0.630	0.000
0.005	0.490	0.580	0.284	0.005	0.490	0.571	0.280
0.010	0.980	0.530	0.519	0.010	0.980	0.524	0.514
0.015	1.471	0.490	0.721	0.015	1.471	0.484	0.711
0.020	1.961	0.457	0.895	0.020	1.961	0.450	0.882
0.025	2.451	0.426	1.043	0.025	2.451	0.420	1.029
0.030	2.941	0.397	1.168	0.030	2.941	0.392	1.151
0.035	3.431	0.371	1.271	0.035	3.431	0.364	1.247
0.040	3.922	0.346	1.355	0.040	3.922	0.339	1.327
0.045	4.412	0.322	1.421	0.045	4.412	0.314	1.383
0.050	4.902	0.299	1.463	0.050	4.902	0.290	1.422
0.055	5.392	0.276	1.488	0.055	5.392	0.266	1.434
0.060	5.882	0.254	1.491	0.060	5.882	0.245	1.438
0.065	6.373	0.233	1.482	0.065	6.373	0.224	1.424
0.070	6.863	0.211	1.448	0.070	6.863	0.201	1.379
0.075	7.353	0.192	1.408	0.075	7.353	0.182	1.335
0.080	7.843	0.170	1.329	0.080	7.843	0.162	1.267
0.085	8.333	0.151	1.254	0.085	8.333	0.142	1.183
0.090	8.824	0.132	1.160	0.090	8.824	0.122	1.076
0.095	9.314	0.110	1.025	0.095	9.314	0.105	0.973
0.100	9.804	0.088	0.863	---	---	---	---

Table F.4: Cell design: membrane – Nafion 117; connector plates – stainless steel; anode catalyst – 3 mg/cm^2 of 40% Pt - 40% Sn/20% CB in 0.190 mm carbon paper; cathode catalyst – 1.0 mg/cm^2 of Pt in 0.400 mm carbon paper.

2M				3M			
Current (A)	Current Density (mA/cm^2)	Voltage (V)	Power Density (mW/cm^2)	Current (A)	Current Density (mA/cm^2)	Voltage (V)	Power Density (mW/cm^2)
0.000	0.000	0.643	0.000	0.000	0.000	0.613	0.000
0.005	0.490	0.604	0.296	0.005	0.490	0.533	0.261
0.010	0.980	0.570	0.558	0.010	0.980	0.478	0.468
0.015	1.471	0.540	0.794	0.015	1.471	0.435	0.639
0.020	1.961	0.512	1.004	0.020	1.961	0.400	0.784
0.025	2.451	0.487	1.194	0.025	2.451	0.370	0.906
0.030	2.941	0.465	1.366	0.030	2.941	0.346	1.016

0.035	3.431	0.443	1.518	0.035	3.431	0.318	1.091
0.040	3.922	0.422	1.655	0.040	3.922	0.295	1.157
0.045	4.412	0.400	1.765	0.045	4.412	0.273	1.202
0.050	4.902	0.381	1.868	0.050	4.902	0.252	1.235
0.060	5.882	0.347	2.041	0.060	5.882	0.215	1.265
0.070	6.863	0.315	2.158	0.070	6.863	0.179	1.228
0.080	7.843	0.283	2.216	0.080	7.843	0.146	1.141
0.090	8.824	0.251	2.210	0.090	8.824	0.112	0.984
0.100	9.804	0.220	2.152	0.100	9.804	0.073	0.711
0.110	10.784	0.191	2.060	---	---	---	---
0.120	11.765	0.161	1.894	---	---	---	---
0.130	12.745	0.131	1.670	---	---	---	---
0.140	13.725	0.096	1.311	---	---	---	---

Appendix G

Effect of binary anode catalyst metal percentages

Table G.1: Cell design: membrane – Nafion 117; connector plates – stainless steel; anode catalyst – 3 mg/cm^2 of 40% Pt - 40% Sn/20% CB in 0.400 mm carbon cloth; cathode catalyst – 1.0 mg/cm^2 of Pt in 0.400 mm carbon paper.

2M				3M			
Current (A)	Current Density (mA/cm^2)	Voltage (V)	Power Density (mW/cm^2)	Current (A)	Current Density (mA/cm^2)	Voltage (V)	Power Density (mW/cm^2)
0.000	0.000	0.637	0.000	0.000	0.000	0.631	0.000
0.005	0.490	0.602	0.295	0.005	0.490	0.603	0.296
0.010	0.980	0.568	0.557	0.010	0.980	0.578	0.566
0.015	1.471	0.537	0.789	0.015	1.471	0.554	0.814
0.020	1.961	0.509	0.998	0.020	1.961	0.531	1.041
0.025	2.451	0.484	1.185	0.025	2.451	0.510	1.250
0.030	2.941	0.460	1.351	0.030	2.941	0.491	1.444
0.035	3.431	0.438	1.501	0.035	3.431	0.472	1.620
0.040	3.922	0.416	1.631	0.040	3.922	0.454	1.780
0.045	4.412	0.395	1.743	0.045	4.412	0.437	1.926
0.050	4.902	0.375	1.838	0.050	4.902	0.420	2.059
0.060	5.882	0.338	1.985	0.060	5.882	0.389	2.288
0.070	6.863	0.302	2.073	0.070	6.863	0.360	2.467
0.080	7.843	0.268	2.102	0.080	7.843	0.331	2.596
0.090	8.824	0.236	2.082	0.090	8.824	0.303	2.674
0.100	9.804	0.205	2.010	0.100	9.804	0.276	2.701
0.110	10.784	0.175	1.887	0.110	10.784	0.248	2.675
0.120	11.765	0.147	1.729	0.120	11.765	0.223	2.618
0.130	12.745	0.120	1.523	0.130	12.745	0.196	2.492
0.140	13.725	0.086	1.174	0.140	13.725	0.169	2.313
---	---	---	---	0.150	14.706	0.141	2.074
---	---	---	---	0.160	15.686	0.114	1.780
---	---	---	---	0.170	16.667	0.085	1.408

Table G.2: Cell design: membrane – Nafion 117; connector plates – stainless steel; anode catalyst – 3 mg/cm^2 of 20% Pt - 20% Sn/60% CB in 0.400 mm carbon cloth; cathode catalyst – 1.0 mg/cm^2 of Pt in 0.400 mm carbon paper.

2M				3M			
Current (A)	Current Density (mA/cm^2)	Voltage (V)	Power Density (mW/cm^2)	Current (A)	Current Density (mA/cm^2)	Voltage (V)	Power Density (mW/cm^2)
0.000	0.000	0.563	0.000	0.000	0.000	0.541	0.000
0.005	0.490	0.405	0.199	0.005	0.490	0.394	0.193
0.010	0.980	0.327	0.320	0.010	0.980	0.322	0.315
0.015	1.471	0.270	0.397	0.015	1.471	0.269	0.396
0.020	1.961	0.224	0.438	0.020	1.961	0.224	0.439
0.025	2.451	0.181	0.444	0.025	2.451	0.187	0.457
0.030	2.941	0.143	0.421	0.030	2.941	0.156	0.459
0.035	3.431	0.108	0.369	0.035	3.431	0.122	0.417
0.040	3.922	0.082	0.320	0.040	3.922	0.089	0.347

Table G.3: Cell design: membrane – Nafion 117; connector plates – stainless steel; anode catalyst – 3 mg/cm^2 of 40% Pt - 40% Sn/20% CB in 0.190 mm carbon paper; cathode catalyst – 1.0 mg/cm^2 of Pt in 0.400 mm carbon paper.

2M				3M			
Current (A)	Current Density (mA/cm^2)	Voltage (V)	Power Density (mW/cm^2)	Current (A)	Current Density (mA/cm^2)	Voltage (V)	Power Density (mW/cm^2)
0.000	0.000	0.643	0.000	0.000	0.000	0.613	0.000
0.005	0.490	0.604	0.296	0.005	0.490	0.533	0.261
0.010	0.980	0.570	0.558	0.010	0.980	0.478	0.468
0.015	1.471	0.540	0.794	0.015	1.471	0.435	0.639
0.020	1.961	0.512	1.004	0.020	1.961	0.400	0.784
0.025	2.451	0.487	1.194	0.025	2.451	0.370	0.906
0.030	2.941	0.465	1.366	0.030	2.941	0.346	1.016
0.035	3.431	0.443	1.518	0.035	3.431	0.318	1.091
0.040	3.922	0.422	1.655	0.040	3.922	0.295	1.157
0.045	4.412	0.400	1.765	0.045	4.412	0.273	1.202
0.050	4.902	0.381	1.868	0.050	4.902	0.252	1.235
0.060	5.882	0.347	2.041	0.060	5.882	0.215	1.265
0.070	6.863	0.315	2.158	0.070	6.863	0.179	1.228
0.080	7.843	0.283	2.216	0.080	7.843	0.146	1.141
0.090	8.824	0.251	2.210	0.090	8.824	0.112	0.984
0.100	9.804	0.220	2.152	0.100	9.804	0.073	0.711
0.110	10.784	0.191	2.060	---	---	---	---
0.120	11.765	0.161	1.894	---	---	---	---
0.130	12.745	0.131	1.670	---	---	---	---
0.140	13.725	0.096	1.311	---	---	---	---

Table G.4: Cell design: membrane – Nafion 117; connector plates – stainless steel; anode catalyst – 3 mg/cm^2 of 20% Pt - 20% Sn/60% CB in 0.190 mm carbon paper; cathode catalyst – 1.0 mg/cm^2 of Pt in 0.400 mm carbon paper.

2M				3M			
Current (A)	Current Density (mA/cm^2)	Voltage (V)	Power Density (mW/cm^2)	Current (A)	Current Density (mA/cm^2)	Voltage (V)	Power Density (mW/cm^2)
0.000	0.000	0.602	0.000	0.000	0.000	0.602	0.000
0.005	0.490	0.446	0.219	0.005	0.490	0.468	0.229
0.010	0.980	0.369	0.362	0.010	0.980	0.395	0.387
0.015	1.471	0.315	0.463	0.015	1.471	0.341	0.501
0.020	1.961	0.271	0.530	0.020	1.961	0.298	0.584
0.025	2.451	0.233	0.571	0.025	2.451	0.262	0.642
0.030	2.941	0.198	0.582	0.030	2.941	0.230	0.675
0.035	3.431	0.165	0.566	0.035	3.431	0.199	0.683
0.040	3.922	0.134	0.525	0.040	3.922	0.171	0.669
0.045	4.412	0.095	0.419	0.045	4.412	0.143	0.631
---	---	---	---	0.050	4.902	0.118	0.576
---	---	---	---	0.055	5.392	0.091	0.491

Appendix H

Effect of anode gas diffusion layer material

Table H.1: Cell design: membrane – Nafion 117; connector plates – stainless steel; anode catalyst – 3 mg/cm^2 of 40% Pt - 40% Sn/20% CB in 0.190 mm carbon paper; cathode catalyst – 1.0 mg/cm^2 of Pt in 0.400 mm carbon paper.

2M				3M			
Current (A)	Current Density (mA/cm^2)	Voltage (V)	Power Density (mW/cm^2)	Current (A)	Current Density (mA/cm^2)	Voltage (V)	Power Density (mW/cm^2)
0.000	0.000	0.643	0.000	0.000	0.000	0.613	0.000
0.005	0.490	0.604	0.296	0.005	0.490	0.533	0.261
0.010	0.980	0.570	0.558	0.010	0.980	0.478	0.468
0.015	1.471	0.540	0.794	0.015	1.471	0.435	0.639
0.020	1.961	0.512	1.004	0.020	1.961	0.400	0.784
0.025	2.451	0.487	1.194	0.025	2.451	0.370	0.906
0.030	2.941	0.465	1.366	0.030	2.941	0.346	1.016
0.035	3.431	0.443	1.518	0.035	3.431	0.318	1.091
0.040	3.922	0.422	1.655	0.040	3.922	0.295	1.157
0.045	4.412	0.400	1.765	0.045	4.412	0.273	1.202
0.050	4.902	0.381	1.868	0.050	4.902	0.252	1.235
0.060	5.882	0.347	2.041	0.060	5.882	0.215	1.265
0.070	6.863	0.315	2.158	0.070	6.863	0.179	1.228
0.080	7.843	0.283	2.216	0.080	7.843	0.146	1.141
0.090	8.824	0.251	2.210	0.090	8.824	0.112	0.984
0.100	9.804	0.220	2.152	0.100	9.804	0.073	0.711
0.110	10.784	0.191	2.060	---	---	---	---
0.120	11.765	0.161	1.894	---	---	---	---
0.130	12.745	0.131	1.670	---	---	---	---
0.140	13.725	0.096	1.311	---	---	---	---

Table H.2: Cell design: membrane – Nafion 117; connector plates – stainless steel; anode catalyst – 3 mg/cm^2 of 40% Pt - 40% Sn/20% CB in 0.400 mm carbon cloth; cathode catalyst – 1.0 mg/cm^2 of Pt in 0.400 mm carbon paper.

2M				3M			
Current (A)	Current Density (mA/cm^2)	Voltage (V)	Power Density (mW/cm^2)	Current (A)	Current Density (mA/cm^2)	Voltage (V)	Power Density (mW/cm^2)
0.000	0.000	0.637	0.000	0.000	0.000	0.631	0.000
0.005	0.490	0.602	0.295	0.005	0.490	0.603	0.296
0.010	0.980	0.568	0.557	0.010	0.980	0.578	0.566
0.015	1.471	0.537	0.789	0.015	1.471	0.554	0.814
0.020	1.961	0.509	0.998	0.020	1.961	0.531	1.041
0.025	2.451	0.484	1.185	0.025	2.451	0.510	1.250
0.030	2.941	0.460	1.351	0.030	2.941	0.491	1.444
0.035	3.431	0.438	1.501	0.035	3.431	0.472	1.620
0.040	3.922	0.416	1.631	0.040	3.922	0.454	1.780
0.045	4.412	0.395	1.743	0.045	4.412	0.437	1.926
0.050	4.902	0.375	1.838	0.050	4.902	0.420	2.059
0.060	5.882	0.338	1.985	0.060	5.882	0.389	2.288
0.070	6.863	0.302	2.073	0.070	6.863	0.360	2.467

0.080	7.843	0.268	2.102	0.080	7.843	0.331	2.596
0.090	8.824	0.236	2.082	0.090	8.824	0.303	2.674
0.100	9.804	0.205	2.010	0.100	9.804	0.276	2.701
0.110	10.784	0.175	1.887	0.110	10.784	0.248	2.675
0.120	11.765	0.147	1.729	0.120	11.765	0.223	2.618
0.130	12.745	0.120	1.523	0.130	12.745	0.196	2.492
0.140	13.725	0.086	1.174	0.140	13.725	0.169	2.313
---	---	---	---	0.150	14.706	0.141	2.074
---	---	---	---	0.160	15.686	0.114	1.780
---	---	---	---	0.170	16.667	0.085	1.408

Table H.3: Cell design: membrane – Nafion 117; connector plates – stainless steel; anode catalyst – 3 mg/cm^2 of 40% Pt - 40% Sn/20% CB in 0.425 mm carbon cloth; cathode catalyst – 1.0 mg/cm^2 of Pt in 0.400 mm carbon paper.

2M				3M			
Current (A)	Current Density (mA/cm^2)	Voltage (V)	Power Density (mW/cm^2)	Current (A)	Current Density (mA/cm^2)	Voltage (V)	Power Density (mW/cm^2)
0.000	0.000	0.638	0.000	0.000	0.000	0.616	0.000
0.005	0.490	0.589	0.288	0.005	0.490	0.543	0.266
0.010	0.980	0.547	0.536	0.010	0.980	0.487	0.477
0.015	1.471	0.512	0.752	0.015	1.471	0.445	0.654
0.020	1.961	0.480	0.941	0.020	1.961	0.411	0.805
0.025	2.451	0.452	1.108	0.025	2.451	0.381	0.933
0.030	2.941	0.427	1.256	0.030	2.941	0.354	1.040
0.035	3.431	0.404	1.385	0.035	3.431	0.327	1.122
0.040	3.922	0.381	1.492	0.040	3.922	0.306	1.198
0.045	4.412	0.360	1.588	0.045	4.412	0.284	1.251
0.050	4.902	0.341	1.669	0.050	4.902	0.264	1.292
0.060	5.882	0.306	1.800	0.060	5.882	0.228	1.338
0.070	6.863	0.275	1.887	0.070	6.863	0.194	1.331
0.080	7.843	0.245	1.918	0.080	7.843	0.163	1.275
0.090	8.824	0.217	1.910	0.090	8.824	0.133	1.169
0.100	9.804	0.188	1.843	0.100	9.804	0.103	1.005
0.110	10.784	0.160	1.725	0.110	10.784	0.069	0.744
0.120	11.765	0.134	1.571	---	---	---	---
0.130	12.745	0.107	1.357	---	---	---	---
0.140	13.725	0.077	1.050	---	---	---	---

Table H.4: Cell design: membrane – Nafion 117; connector plates – stainless steel; anode catalyst – 3 mg/cm^2 of 40% Pt - 40% Sn/20% CB in 0.110 mm carbon paper; cathode catalyst – 1.0 mg/cm^2 of Pt in 0.400 mm carbon paper.

2M				3M			
Current (A)	Current Density (mA/cm^2)	Voltage (V)	Power Density (mW/cm^2)	Current (A)	Current Density (mA/cm^2)	Voltage (V)	Power Density (mW/cm^2)
0.000	0.000	0.639	0.000	0.000	0.000	0.629	0.000
0.005	0.490	0.591	0.290	0.005	0.490	0.579	0.284
0.010	0.980	0.547	0.536	0.010	0.980	0.533	0.522
0.015	1.471	0.509	0.749	0.015	1.471	0.495	0.728
0.020	1.961	0.476	0.933	0.020	1.961	0.463	0.907
0.025	2.451	0.445	1.091	0.025	2.451	0.430	1.054
0.030	2.941	0.416	1.224	0.030	2.941	0.401	1.178

0.035	3.431	0.389	1.335	0.035	3.431	0.372	1.276
0.040	3.922	0.362	1.420	0.040	3.922	0.343	1.345
0.045	4.412	0.336	1.482	0.045	4.412	0.316	1.392
0.050	4.902	0.312	1.529	0.050	4.902	0.289	1.414
0.060	5.882	0.270	1.588	0.060	5.882	0.248	1.456
0.070	6.863	0.228	1.565	0.070	6.863	0.195	1.338
0.080	7.843	0.166	1.302	0.080	7.843	0.156	1.220
0.090	8.824	0.121	1.068	0.090	8.824	0.116	1.019
0.100	9.804	0.072	0.706	0.100	9.804	0.074	0.721

Appendix I

Effect of binary anode catalyst metal percentage keeping an overall metal percentage of 40%

Table I.1: Cell design: membrane – Nafion 117; connector plates – stainless steel; anode catalyst – 3 mg/cm^2 of 20% Pt - 20% Sn/60% CB (50% Pt- 50% Sn for an overall metal percentage of 40%) in 0.400 mm carbon cloth; cathode catalyst – 1.0 mg/cm^2 of Pt in 0.400 mm carbon paper.

2M				3M			
Current (A)	Current Density (mA/cm^2)	Voltage (V)	Power Density (mW/cm^2)	Current (A)	Current Density (mA/cm^2)	Voltage (V)	Power Density (mW/cm^2)
0.000	0.000	0.563	0.000	0.000	0.000	0.541	0.000
0.005	0.490	0.405	0.199	0.005	0.490	0.394	0.193
0.010	0.980	0.327	0.320	0.010	0.980	0.322	0.315
0.015	1.471	0.270	0.397	0.015	1.471	0.269	0.396
0.020	1.961	0.224	0.438	0.020	1.961	0.224	0.439
0.025	2.451	0.181	0.444	0.025	2.451	0.187	0.457
0.030	2.941	0.143	0.421	0.030	2.941	0.156	0.459
0.035	3.431	0.108	0.369	0.035	3.431	0.122	0.417
0.040	3.922	0.082	0.320	0.040	3.922	0.089	0.347

Table I.2: Cell design: membrane – Nafion 117; connector plates – stainless steel; anode catalyst – 3 mg/cm^2 of 24% Pt - 16% Sn/60% CB (60% Pt- 40% Sn for an overall metal percentage of 40%) in 0.400 mm carbon cloth; cathode catalyst – 1.0 mg/cm^2 of Pt in 0.400 mm carbon paper.

2M				3M			
Current (A)	Current Density (mA/cm^2)	Voltage (V)	Power Density (mW/cm^2)	Current (A)	Current Density (mA/cm^2)	Voltage (V)	Power Density (mW/cm^2)
0.000	0.000	0.644	0.000	0.000	0.000	0.631	0.000
0.005	0.490	0.595	0.292	0.005	0.490	0.594	0.291
0.010	0.980	0.553	0.542	0.010	0.980	0.559	0.548
0.015	1.471	0.516	0.759	0.015	1.471	0.528	0.776
0.020	1.961	0.484	0.948	0.020	1.961	0.500	0.979
0.025	2.451	0.455	1.114	0.025	2.451	0.472	1.156
0.030	2.941	0.428	1.257	0.030	2.941	0.446	1.312
0.035	3.431	0.404	1.386	0.035	3.431	0.422	1.446
0.040	3.922	0.380	1.488	0.040	3.922	0.397	1.555
0.045	4.412	0.356	1.568	0.045	4.412	0.381	1.679
0.050	4.902	0.333	1.632	0.050	4.902	0.360	1.762
0.060	5.882	0.286	1.679	0.060	5.882	0.322	1.894
0.070	6.863	0.253	1.736	0.070	6.863	0.288	1.973
0.080	7.843	0.218	1.710	0.080	7.843	0.254	1.988
0.090	8.824	0.184	1.624	0.090	8.824	0.220	1.941
0.100	9.804	0.151	1.475	0.100	9.804	0.188	1.838
0.110	10.784	0.114	1.224	0.110	10.784	0.154	1.655
0.120	11.765	0.084	0.982	0.120	11.765	0.124	1.453
---	---	---	---	0.130	12.745	0.090	1.141

Appendix J

Effect of ternary anode catalyst metals

Table J.1: Cell design: membrane – Nafion 117; connector plates – stainless steel; anode catalyst – 3 mg/cm^2 of 24% Pt - 16% Sn/60% (60% Pt- 40% Sn for an overall metal percentage of 40%) in 0.400 mm carbon cloth; cathode catalyst – 1.0 mg/cm^2 of Pt in 0.400 mm carbon paper.

2M				3M			
Current (A)	Current Density (mA/cm^2)	Voltage (V)	Power Density (mW/cm^2)	Current (A)	Current Density (mA/cm^2)	Voltage (V)	Power Density (mW/cm^2)
0.000	0.000	0.644	0.000	0.000	0.000	0.631	0.000
0.005	0.490	0.595	0.292	0.005	0.490	0.594	0.291
0.010	0.980	0.553	0.542	0.010	0.980	0.559	0.548
0.015	1.471	0.516	0.759	0.015	1.471	0.528	0.776
0.020	1.961	0.484	0.948	0.020	1.961	0.500	0.979
0.025	2.451	0.455	1.114	0.025	2.451	0.472	1.156
0.030	2.941	0.428	1.257	0.030	2.941	0.446	1.312
0.035	3.431	0.404	1.386	0.035	3.431	0.422	1.446
0.040	3.922	0.380	1.488	0.040	3.922	0.397	1.555
0.045	4.412	0.356	1.568	0.045	4.412	0.381	1.679
0.050	4.902	0.333	1.632	0.050	4.902	0.360	1.762
0.060	5.882	0.286	1.679	0.060	5.882	0.322	1.894
0.070	6.863	0.253	1.736	0.070	6.863	0.288	1.973
0.080	7.843	0.218	1.710	0.080	7.843	0.254	1.988
0.090	8.824	0.184	1.624	0.090	8.824	0.220	1.941
0.100	9.804	0.151	1.475	0.100	9.804	0.188	1.838
0.110	10.784	0.114	1.224	0.110	10.784	0.154	1.655
0.120	11.765	0.084	0.982	0.120	11.765	0.124	1.453
---	---	---	---	0.130	12.745	0.090	1.141

Table J.2: Cell design: membrane – Nafion 117; connector plates – stainless steel; anode catalyst – 3 mg/cm^2 of 24% Pt - 12% Sn - 4% Ni/60% CB (60% Pt- 30% Sn - 10% Ni for an overall metal percentage of 40%) in 0.400 mm carbon cloth; cathode catalyst – 1.0 mg/cm^2 of Pt in 0.400 mm carbon paper.

2M				3M			
Current (A)	Current Density (mA/cm^2)	Voltage (V)	Power Density (mW/cm^2)	Current (A)	Current Density (mA/cm^2)	Voltage (V)	Power Density (mW/cm^2)
0.000	0.000	0.650	0.000	0.000	0.000	0.639	0.000
0.005	0.490	0.600	0.294	0.005	0.490	0.593	0.291
0.010	0.980	0.556	0.545	0.010	0.980	0.551	0.540
0.015	1.471	0.517	0.760	0.015	1.471	0.514	0.755
0.020	1.961	0.483	0.947	0.020	1.961	0.478	0.937
0.025	2.451	0.456	1.118	0.025	2.451	0.449	1.099
0.030	2.941	0.429	1.262	0.030	2.941	0.422	1.241
0.035	3.431	0.404	1.385	0.035	3.431	0.394	1.352
0.040	3.922	0.379	1.484	0.040	3.922	0.371	1.455
0.045	4.412	0.352	1.551	0.045	4.412	0.343	1.513
0.050	4.902	0.324	1.588	0.050	4.902	0.319	1.561
0.060	5.882	0.279	1.641	0.060	5.882	0.274	1.612

0.070	6.863	0.236	1.616	0.070	6.863	0.237	1.626
0.080	7.843	0.196	1.533	0.080	7.843	0.197	1.541
0.090	8.824	0.162	1.429	0.090	8.824	0.158	1.390
0.100	9.804	0.130	1.275	0.100	9.804	0.122	1.196
0.110	10.784	0.094	1.014	0.110	10.784	0.089	0.960

Table J.3: Cell design: membrane – Nafion 117; connector plates – stainless steel; anode catalyst – 3 mg/cm^2 of 24% Pt - 12% Sn - 4% Co/60% CB (60% Pt- 30% Sn - 10% Co for an overall metal percentage of 40%) in 0.400 mm carbon cloth; cathode catalyst – 1.0 mg/cm^2 of Pt in 0.400 mm carbon paper.

2M				3M			
Current (A)	Current Density (mA/cm^2)	Voltage (V)	Power Density (mW/cm^2)	Current (A)	Current Density (mA/cm^2)	Voltage (V)	Power Density (mW/cm^2)
0.000	0.000	0.571	0.000	0.000	0.000	0.577	0.000
0.005	0.490	0.447	0.219	0.005	0.490	0.450	0.221
0.010	0.980	0.380	0.373	0.010	0.980	0.383	0.375
0.015	1.471	0.327	0.481	0.015	1.471	0.329	0.484
0.020	1.961	0.282	0.553	0.020	1.961	0.282	0.553
0.025	2.451	0.241	0.589	0.025	2.451	0.241	0.589
0.030	2.941	0.202	0.593	0.030	2.941	0.202	0.594
0.035	3.431	0.164	0.563	0.035	3.431	0.165	0.564
0.040	3.922	0.126	0.494	0.040	3.922	0.129	0.504
0.045	4.412	0.082	0.362	0.045	4.412	0.094	0.415